Drug Design, Development and Therapy

Dovepress
open access to scientific and medical research

Open Access Full Text Article

ORIGINAL RESEARCH

An Integrated Analysis of Network Pharmacology, Molecular Docking, and Experiment Validation to Explore the New Candidate Active Component and Mechanism of *Cuscutae Semen-Mori Fructus* Coupled-Herbs in Treating Oligoasthenozoospermia

Xue Bai,[1] Yibo Tang,[2] Qiang Li,[1] Dan Liu,[1] Guimin Liu,[1] Xiaolei Fan,[2] Zhejun Liu,[2] Shujun Yu,[1] Tian Tang,[1] Shuyan Wang,[2] Lingru Li,[3] Kailin Zhou,[4] Yanfei Zheng,[3] Zhenquan Liu[1,3]

[1]School of Chinese Materia Medica, Beijing University of Chinese Medicine, Beijing, People's Republic of China; [2]School of Traditional Chinese Medicine, Beijing University of Chinese Medicine, Beijing, People's Republic of China; [3]National Institute of TCM Constitution and Preventive Medicine, Beijing University of Chinese Medicine, Beijing, People's Republic of China; [4]School of Humanities, Beijing University of Chinese Medicine, Beijing, People's Republic of China

Correspondence: Yanfei Zheng
National Institute of TCM Constitution and Preventive Medicine, Beijing University of Chinese Medicine, Beijing, People's Republic of China
Tel +8618010091957
Email yanfei_z@163.com

Zhenquan Liu
School of Chinese Materia Medica, National Institute of TCM Constitution and Preventive Medicine, Beijing University of Chinese Medicine, Beijing, People's Republic of China
Tel +86 13810419708
Email lzqbzy@sina.com

Purpose: One of the most common types of male infertility is recognized as oligoasthenozoospermia (OA), characterized by low sperm count and quality in males. As a traditional Chinese medicine (TCM), *Cuscutae Semen-Mori Fructus* coupled-herbs (CSMFCH) has been known to act a curative effect on OA for thousands of years. Nevertheless, the substantial basis and molecular mechanism of CSMFCH in treating OA remain elusive.

Methods: Herein, an integrated approach, including network pharmacology, molecular docking, and experiment validation, was utilized to reveal the new candidate active component and mechanism of CSMFCH in treating OA.

Results: The results show that kaempferol is the most significant bioactive component of CSMFCH on OA. The mechanism and targets of CSMFCH against OA are relevant to hormone regulation, oxidant stress, and reproductive promotion. In order to validate network pharmacology results, molecular docking and experiment validation were conducted. In detail, molecular docking was employed to verify the strong binding interactions between kaempferol and the core targets. UHPLC-Q-Orbitrap-MS was used to identify kaempferol in the CSMFCH extract. In vitro and in vivo experiments further proved CSMFCH and kaempferol could enhance the mouse Leydig (TM3) and mouse Sertoli (TM4) cell viability, improve the male reproductive organ weights, sperm quality, and decrease testis tissue damage in the OA mouse model induced by CP.

Conclusion: Our results not only identify the new candidate active component of CSMFCH in treating OA but also provide new insights into the mechanisms of CSMFCH against OA.

Keywords: traditional Chinese medicine, oligoasthenozoospermia, kaempferol, network pharmacology

Introduction

Infertility affects nearly 60 to 80 million couples worldwide, which is defined as the inability to conceive after 12 months of regular unprotected intercourse.[1] Male infertility accounts for almost half of the infertility cases.[2] Oligoasthenozoospermia (OA) is clearly amongst the most common forms of male infertility, which arises

Received: 18 February 2021
Accepted: 20 April 2021
Published: 17 May 2021

under circumstances that the total sperm number or sperm concentration of gradually mobile sperm are below the lower reference limits (total number < 39×10^6 per ejaculate; concentration < 15×10^6 per mL; progressively motile < 32%).[3,4] Earlier studies have shown that a significant range of factors affect sperm production, including varicocele, idiopathic, obstruction, cryptorchidism, immunological, ejaculatory, testicular insufficient, medicinal/radioactive, endocrinological, etc., which may further prompt the occurrence of OA.[5] Moreover, the aetiology remains unknown in one-third of all OA patients.[6] To be noted, recent studies have demonstrated that sperm concentration and motility decreased for 72–90 days following Coronavirus Disease 2019 (COVID-19) infection.[7–10] Moreover, high fever in COVID-19 patients could lead to germ cell destruction and testicular dysfunction, inducing OA.[11–13] Thus, more attention should be paid to the treatment of OA to meet the rising demand. However, the pathological mechanism of OA remains unclear, and the current treatment has poor therapeutic effects and limitations.[14,15] Medicines available to treat OA are clomiphene citrate, vitamin E, L-Carnitine, etc., but they still have some limitations.[16] For example, a double-blind randomized controlled trial showed that clomiphene citrate did not significantly improve the quality of male semen.[17] Although vitamin E could improve the sperm quality, there is no uniform standard for usage.[18] Clinically, vitamin E is generally not used alone but often combined with other drugs, such as Traditional Chinese Medicine (TCM), to improve sperm parameters.[19] Moreover, L-Carnitine treatment could not significantly improve the sperm motility or fertility in a high-fat diet (HFD)-induced obesity mouse model.[20] Especially for unexplained idiopathic OA, there is no effective treatment yet.[14,15] For instance, as a widely accepted technology on infertility, assisted reproductive technology (ART) could improve the pregnancy rate of infertile couples.[21] However, some problems of ART are still unsolved, such as associated high-cost, potential risk to safety, uncertainty about treatment. Besides, ART could not fundamentally improve the sperm count and quality of OA patients. Thus, developing new therapy or drug to cure OA is essential.

For thousands of years, TCM has been used to treat male infertility, including OA.[22] The most essential feature of TCM is employing multiple components for multiple targets to produce therapeutic efficacies. Given the complex pathological mechanisms of OA, the multiple targets strategy of TCM is considered to act as a positive effect to prevent the development of OA. *Cuscutae Semen-Mori Fructus* coupled-herbs (CSMFCH), composed of *Cuscutae Semen* (CS) and *Mori Fructus* (MF), has a long medicinal history and occurs frequently in anti-OA Chinese patent medicine (CPM), such as Qilin Pill[23] and Shengjing Capsule.[24] CS could regulate the endocrine system and immune system and has anti-aging and anti-tumor effects.[25–28] MF has many biological activities including immunomodulation, antitumor, hypoglycemic and hypolipidemic effects.[29–31] However, the unclear molecular mechanism of CSMFCH against OA greatly limits its clinical application. Therefore, it is of importance to reveal the bioactive components and potential targets of CSMFCH in the treatment of OA.

The emerging network pharmacology approach offers a new viewpoint to elucidate the molecular mechanism of the network between component-target and target-disease, which is compatible with the "multi-component" and "multi-target" characteristics of TCM.[32,33] Herein, we proposed a novel strategy combining network pharmacology approach,[34,35] molecular docking,[36] UHPLC-Q-Orbitrap-MS analysis, in vitro and in vivo experiments to explore the new candidate active component and mechanism of CSMFCH against OA. Based on data screening, protein–protein interaction (PPI) network, cluster analysis, enrichment of Gene Ontology (GO) and Kyoto Encyclopedia of Genes and Genomes (KEGG), we constructed the core component-target pathway network. Thus, the new candidate active component and mechanism of CSMFCH in treating OA were predicted. Furthermore, UHPLC-Q-Orbitrap-MS analysis was used to identify the new candidate active component. In vitro and in vivo experiments was conducted to investigate the effects of the new candidate active component and CSMFCH on OA.

Materials and Methods

CSMFCH Component-Targets and Network

To screen the components of CSMFCH, two frequently used databases, TCMSP (http://tcmspw.com/tcmsp.php)[37] and TCMID (http://119.3.41.228:8000/tcmid/),[38] were employed to collect the components of CHMFCH (Table S1). According to the published literature,[39–42] two ADME-related models,[43,44] oral bioavailability (OB) ≥ 30% and drug-likeness (DL) ≥ 0.18,[39] were used as the condition to screen the bioactive components by Venn diagram[45] (Table S2). PubChem (https://pubchem.ncbi.

nlm.nih.gov/)[46] and ALOGPS2.1 (http://www.vcclab.org/lab/alogps/)[47] were utilized to obtain the structure information of the bioactive components, such as molecular structures and canonical smiles. Then, the targets of bioactive components were predicted by Swiss Target Prediction (http://www.swisstargetprediction.ch/),[48] with the species limited to "Homo sapiens" and probability value > 0. Finally, the target names were standardized by UniProtKB (https://www.uniprot.org/)[49] (Table S3). The component-target network was then constructed by Cytoscape (http://www.cytoscape.org, version 3.8.0).[50] The Network Analyzer[51] was used for calculating the degree value of node.

OA-Related Targets

In order to identify the OA-related targets, we used five different databases, namely DisGeNET database (https://www.disgenet.org/),[52] Comparative Toxicogenomics Database (CTD, http://ctdbase.org/),[53] Online Mendelian Inheritance in Man (OMIM, http://omim.org/),[54] GeneCards (https://www.genecards.org/, updated on Mar. 11, 2020)[55] and the National Centre for Biotechnology Information Gene (NCBI Gene, https://www.ncbi.nlm.nih.gov/gene/).[56] According to the guidelines of the World Health Organization (WHO), OA is a condition that oligospermia and asthenozoospermia occur simultaneously.[57] Accordingly, we chose "oligoasthenozoospermia", "oligospermia", "oligozoospermia", "asthenospermia" and "asthenozoospermia" as the keywords to search for OA-related targets. Duplicated targets of "oligospermia" and "oligozoospermia" were integrated, and the obtained targets were defined as the oligospermia-related targets. Similarly, the same targets of "asthenospermia" and "asthenozoospermia" were incorporated, and the obtained targets were defined as the asthenozoospermia-related targets. Afterwards, we took the intersection of the oligospermia-related targets and the asthenozoospermia-related targets, and the targets searched by "oligoasthenozoospermia" were added to get the OA-related targets by Venn diagram. In the following analysis, OA-related targets were obtained after standardizing the target names using UniProtKB to examine the interaction between targets and diseases from various perspectives (Table S5).

CSMFCH-OA Common-Target Network

After screening the common targets of CSMFCH and OA by Venn diagram (Table S6), we constructed a CSMFCH-OA common-target network by Cytoscape. The Network Analyzer, a plugin of Cytoscape, were used to evaluate the topological properties of the network (Table S7).

PPI Network

STRING database v11.0 (http://string-db.org)[58] was used to obtain the PPI information of the common targets from CSMFCH and OA. The confidence score was set 0.4 or higher to screen the highly reliable data. The PPI network was visualized by Cytoscape after the PPI information was imported in TSV format. Next, Network Analyzer was utilized to calculate the network topology parameters, in which the network was treated as undirected (Table S9).

Cluster Analysis

We conducted Multi Contrast Delayed Enhancement (MCODE),[59] a cluster analysis algorithm in Cytoscape, to identify nodes with the same or close characteristics as clusters owing to the complexity of the PPI networks[60] (Table S10). Node score cutoff=0.2, K-core=2 and degree of cutoff=2 were set as the conditions.

GO and KEGG Pathway Enrichment Analyses

The bioinformatic analysis of different proteins was performed with GO enrichment (http://geneontology.org/),[61] and KEGG pathway analysis (https://www.genome.jp/kegg/)[62]. Metascape (https://metascape.org/gp/index.html#/main/step1),[63] a R 4.0.0 software with the Bioconductor package,[64] and the ClueGO plug-in (http://apps.cytoscape.org/apps/cluego)[65] were utilized to obtain the results (Table S4, S6, S11-S15).

Molecular Docking

Protein Data Bank (PDB) (http://www.rcsb.org/)[66] was used to obtain the X-ray crystal structures of the targets, including AKT1 (PDB ID:3QKK), EGFR (PDB ID: 5X2K), MAPK3 (PDB ID:6GES), ESR1 (PDB ID:4PXM), CYP19A1 (PDB ID: 3S7S), and AR (PDB ID: 2Q7K). PyMOL 2.4 (https://pymol.org/2/)[67] was then used to eliminate water molecules and pro-ligand small molecules. The protein receptor files and ligand files were processed, and then converted to pdbqt format using AutoDock Tools 1.5.6. Each grid box was centered on ligand. And then, Autodock Vina 1.1.2 was used to perform molecular docking calculations and their affinity.[68] The best affinity conformation was chosen as the final docking conformation. By using PyMOL 2.4 and ligplus,

the docking experiments were visualized and presented as 3D diagrams and 2D diagrams.

Preparation of CSMFCH Extract

CS and MF were purchased from Beijing Tongrentang Pharmacy (Beijing, China). The extract of CSMFCH was prepared as follows:[69,70] (1) 10g CS and 10g MF samples were infused with 140 mL of water for 30 min, then decocted in a stewpot for 2 h at 100 °C. (2) The solution was filtered, and the obtained residue was then decocted with 140 mL of water twice for 2 h. (3) All the filtrate were combined and concentrated to obtain CSMFCH extract (1.29g/mL). (4) The CSMFCH extract was stored at 4 °C for further use.

UHPLC-Q-Orbitrap-MS Analysis

A Thermo fisher U3000 ultra-high performance liquid chromatography (UHPLC) was conducted with the LC-ESI-MS/MS analysis. UHPLC was equipped with an online degassing device, quaternary gradient pump, column temperature chamber, automated sampler, and Q Exactive PlusTM Orbitrap MS (Thermo Scientific, Waltham, MA, USA) system with a source of heated electrospray ionization (HESI). The chromatographic separation was conducted by using Waters ACQUITY UPLC HSS T3 C18 column (2.1 mm × 100 mm, 1.8 μm; Waters Corporation, Milford, MA, USA). A U3000 3D field DAD detector with wavelength ranges from 200 nm to 400 nm was used for UV detection of UHPLC fractions. The analytical column was held at 30°C with an injection volume of 5μL. Gradient elution was carried out with water with 0.1% (v/v) formic acid in water (solvent B) and acetonitrile (solvent A). The flow rate was 0.2 mL/min, and gradient elution was as follows: 0–10 min, 100% B; 10–20 min, 100–70% B; 20–25 min, 70–60% B; 25–30 min, 60–50% B; 30–40 min, 50–30% B; 40–45 min, 30–0% B; 45–60 min, 0%B; 60–60.1 min, 0–100% B; 60.1–70 min, 100% B. For the MS study, positive and negative ion modes were placed in the range of m/z 100–1500. Sheath gas flow of 40 arb, auxiliary gas flow rate of 15 arb, capillary temperature of 320 °C, aux gas heater temperature of 350 °C, positive spray voltage of 3.2 kv were other working MS parameters. The MS resolution is 70,000, and the MS/MS resolution is 17,500. Compound discover 3.1.0.305, with mzcloud and mzVault databases, conducted the discovery of the unknown compounds. In addition, MS/MS spectra of unknown compounds were analyzed with the Thermo Xcalibur Qual Browser using PubChem database (https://pubchem.ncbi.nlm.nih.gov/).[71]

TM3 and TM4 Cell Culture

The TM3 and TM4 cell lines were purchased from the Cell Resource Center, Peking Union Medical College (which is the headquarters of the National Infrastructure of Cell Line Resource). The cell lines were maintained in DMEM/F-12 with 15 mM HEPES and L-glutamine and enriched with 2.5% fetal bovine serum and 5% horse serum in 5% CO_2 incubator at 37°C. The related materials were purchased from the National Infrastructure of Cell Line Resource (Beijing, China) or Sigma-Aldrich (St. Louis, MO, USA).

Cell Proliferation Assays

Cell viability was monitored with CCK-8 kit (CCK-8, Dojindo, Japan) following the producer's suggestions. The TM3 and TM4 cells were cultivated in 96-well plates with six replicate wells with an initial cell density of 5×10^4/well for 24h. Then, the cells were treated with CSMFCH extract and kaempferol for 24h. After that, the medium was discarded and the cells were washed with PBS in order to remove the effects of CSMFCH extract and kaempferol on the absorbance. Each well was added to 100 μL DMEM/F12 culture medium containing 10 μL CCK-8 solution and incubated at 37 °C for 45 min. Meanwhile, a blank well was set to contain no cells but have DMEM/F12 medium and CCK-8 solution. The absorbance was measured using a microplate reader with a wavelength of 450 nm. The proliferative activity was calculated with the formula below: (OD (sample) - OD (blank))/(OD (control) - OD (blank)).

Animals

A total of 36 Kunming male mice weighing 22–25 g were obtained from Vital River Laboratory Animal Technology Co., Ltd. (Beijing, China). The mice were acclimatized to standard housing conditions, including ambient temperature of 23 ± 2 °C, relative humidity at 60% ± 5%, and a 12-h light-dark cycle. The experimental protocols and ethics were approved by the Institutional Animal Care and Use Committee of Beijing University of Chinese Medicine.

Oligoasthenozoospermia Model

The mice model of OA was established according to previous experiments[72–75] by intragastrical administration of cyclophosphamide (CP) once daily for 5 days at a dose of

60 mg/kg/d. The mice exhibited the characteristics of OA in terms of sperm quality and testicular pathology.[73,76]

Experimental Groups, Treatment, and Sample Preparation

The animals were randomly divided into six groups containing 6 mice each. Physiological saline was continuously administered in the normal control (NC) group. The other 5 groups comprised the model control (MC), kaempferol, low-, medium-, and high-dose CSMFCH groups. In the present study, the medium dose for the mice was calculated according to the conversion principle of mice dose to human equivalent dose (HED) based on body surface area. These groups were first intraperitoneally administered with CP to induce OA, followed by physiological saline in the model control group, 12.9 g/kg CSMFCH in the low-dose CSMFCH group, 25.8 g/kg CSMFCH in the medium-dose CSMFCH group, and 51.6 g/kg CSMFCH in the high-dose CSMFCH group once daily for 21 days. All groups were administered a single dose via oral gavage in a volume of 20 mL/kg. After the final treatment, the mice were weighed and anesthetized with CO_2, and their left testes and epididymides were removed by laparotomy and weighed.

Analysis of Sperm Quality

The epididymal tissue of rats was removed and transferred to a 2 mL Eppendorf tube. Then, 1 mL M199 (Hyclone; South Logan, UT) was added to the tube, and the epididymal tissue was cut into small pieces and placed in a warm water bath at 37°C for 30 min. After the sperms in the epididymis were released, sperm quality was tested using the semen analysis system under BK-FL fluorescence microscope (Chongqing Optec Instrument, Chongqing, China). The main indices were sperm density ($\times 10^6$/mL), sperm viability (%), sperm motility (a + b %), and abnormal sperm motility (%).[77]

Histopathological Analysis

Testis tissue was fixed in 4% paraformaldehyde for 24 h, routinely processed with an automatic tissue processor, dehydrated, embedded in paraffin, sectioned at 5-μm, and stained with hematoxylin and eosin (H&E). Cell morphology was observed under a microscope (Jiangsu Kaiji Biotech., China).

Statistical Analysis

The data are expressed as mean ± SD. Comparisons of multiple groups and pairwise comparisons were performed using one-way analysis of variance (ANOVA) with GraphPad software (version 8.0). $P < 0.05$ was considered statistically significant.

Results

CSMFCH Component-Target Network

We obtained 137 components of CSMFCH from TCMSP and TCMID after deleting the same components. Of these, 34 components were from CS, 108 components were from MF, and 5 common components were from CS and MF (Table S1). According to OB ≥ 30% and DL ≥ 0.18 requirements, we retained 18 bioactive components of CSMFCH after removing duplicates. Among them, 13 components come from CS, 8 components come from MF, and 3 common components (quercetin, kaempferol, beta-sitosterol) come from CS and MF (Figure 1A). Next, PubChem and ALOGPS2.1 were provided with structural details for the bioactive components (Table S2). Subsequently, Swiss Target Prediction and SEA were used to predict 306 effective targets from 17 bioactive components of CSMFCH, except cyanin (Table S3). Among these, 153 overlapping targets were from CS and MF, which means that CS and MF have the same or similar interactions with each other. We then constructed CS component-target network (Figure 1B) and MF component-target network (Figure 1C). The CSMFCH component-target network (Figure 1D) was obtained by merging the above networks. The larger the value of the degree is, the more essential the node is.

GO and KEGG Pathway Enrichment Analyses of the CSMFCH Component-Target Network

In attempt to elucidate the essential roles of the OA-related targets, GO and KEGG enrichment analysis were carried out (Table S4). The PPI network was formed by 306 proteins obtained from CSMFCH component-target network, and 9 different clusters were divided by MCODE (Figure 2A and B). Then, KEGG pathway analysis was applied to each MCODE independently, and the three best-scoring terms screened by p-value were retained as the functional description of the corresponding MCODE (Table 1). GO analysis comprises biological process

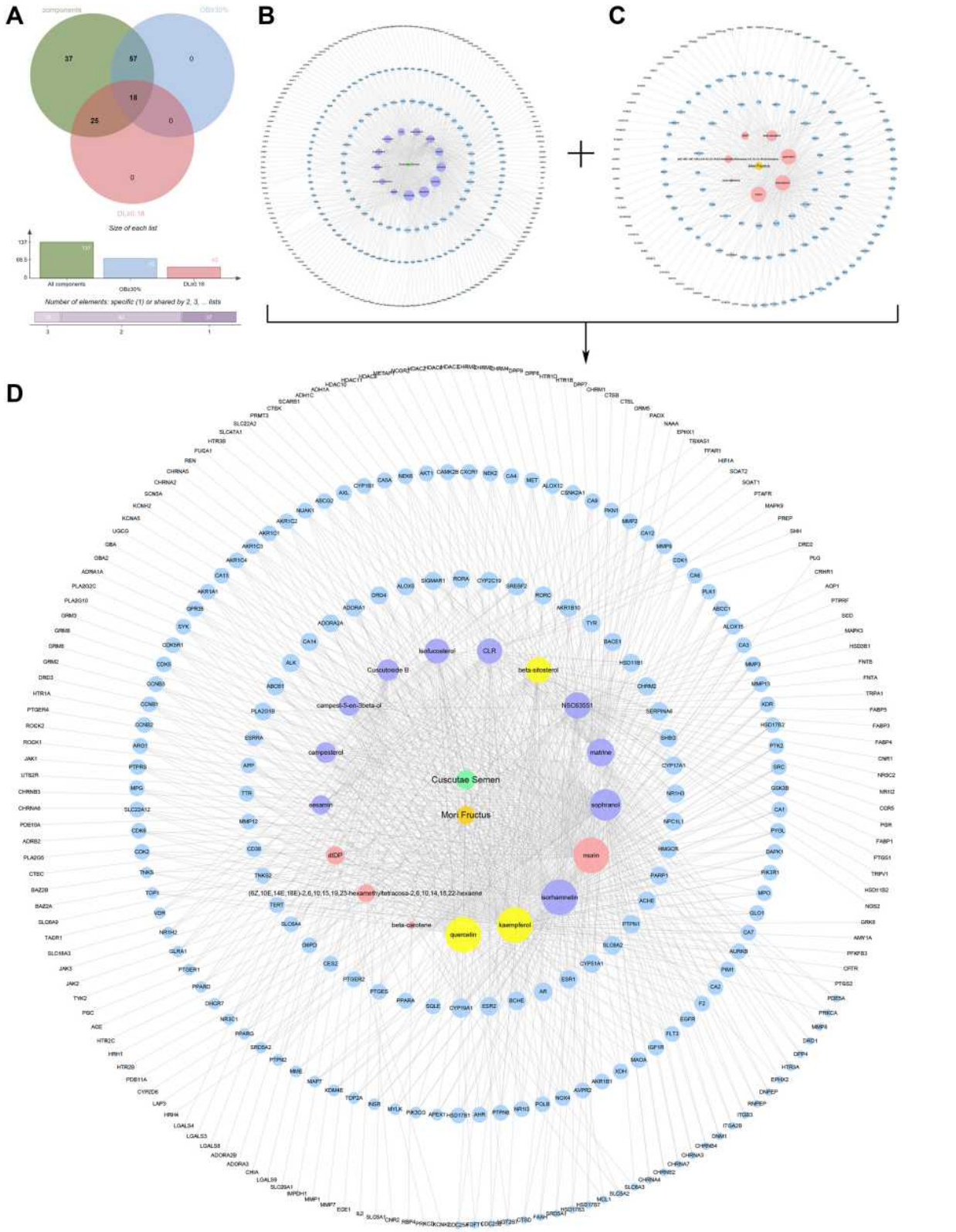

Figure 1 CSMFCH component-target network. (**A**) Venn diagram: 137 components (green section), and 18 bioactive components filtered by two models relevant to ADME (blue section stands for the components of OB ≥ 30%, red section stands for DL ≥ 0.18). (**B**) CS component-target network, including 316 nodes and 714 edges. (**C**) MF component-target network, including 165 nodes and 373 edges. (**D**) Construction of CSMFCH component-target visual network, including 325 nodes and 835 edges. Turquoise node and orange node stand for CS and MF, respectively. Purple nodes and pink nodes stand for bioactive components from CS and MF, respectively. Yellow node stands for the common components from CS and MF. Blue nodes stand for targets.

Abbreviations: CS, *Cuscutae Semen*; MF, *Mori Fructus*; CSMFCH, *Cuscutae Semen-Mori Fructus* coupled-herbs.

(BP), cellular component (CC), and molecular function (MF), which are shown in Figure 2C–E. The top 3 BP terms are trans-synaptic signaling (GO:0099537), cellular response to hormone stimulus (GO:0032870), and regulation of hormone levels (GO:0010817), indicating that CSMFCH is mainly associated with hormone regulation. Moreover, steroid metabolic process (GO:0008202), regulation of lipid metabolic process (GO:0019216), regulation of small molecule metabolic process (GO:0062012), icosanoid metabolic process (GO:0006690), and ammonium ion metabolic process (GO:0097164) terms in BP enrichment imply that CSMFCH has a positive effect on human body through regulating the metabolic process. In addition, circulatory system process (GO:0003013), regulation of secretion by cell (GO:1903530), and regulation of body fluid levels (GO:0050878) show that CSMFCH could improve physical health through regulating circulatory, secretion, and body fluid processes (Figure 2C). The top 3 CC terms are postsynaptic membrane (GO:0045211), dopaminergic synapse (GO:0098691), and membrane raft (GO:0045121), indicating that CSMFCH is mainly associated with hormone regulation. It means that CSMFCH mainly acts on the synaptic membrane in cellular (Figure 2D). Protein kinase activity (GO:0004672), protein tyrosine kinase activity (GO:0004713), histone kinase activity (GO:0035173), oxidoreductase activity (GO:0016491), oxidoreductase activity, acting on paired donors, with incorporation or reduction of molecular oxygen (GO:0016705) in MF reveal that CSMFCH acts an effect on protein kinase and oxidoreductase activities (Figure 2E). The results of KEGG pathway indicate that CSMFCH implements reproductive functions mainly through steroid hormone biosynthesis (hsa00140), progesterone-mediated oocyte maturation (hsa04914), steroid biosynthesis (hsa00100) (Figure 2F). Besides, Table 1 shows that the targets of CSMFCH mainly regulates cell proliferation and differentiation (hsa04914, hsa04110, hsa04114), and synthesis of reproductive hormone (hsa04919, hsa00140, hsa00140, hsa01521). In summary, we assume that CSMFCH could treat disease through regulating hormone, improving reproductive function, and promoting cell proliferation.

OA-Related Targets

OA is a complex disease affected by many proteins, but the underly mechanism is still unclear. Thus, it is necessary to research the relationship between the proteins. As OA is a disease when oligospermia and asthenozoospermia occur simultaneously, we collected 993 and 683 targets from oligospermia and asthenozoospermia, respectively. 473 overlapping targets were obtained by taking the intersection of two arrays. Using "oligoasthenozoospermia" as the supplementary searching term, we finally got 495 (464+9+6+15+1) targets as OA-related targets (Figure 3A). To ensure the comprehensive of the OA-related targets, all data come from five different databases, namely CTD, GeneCards, DisGeNET, OMIM, and NCBI. The number of these targets is 415, 78, 51, 36, and 30, respectively (Figure 3B). Especially, androgen receptor (AR) is the only common gene from the five databases, which we should pay more attention.

GO and KEGG Pathway Enrichment Analyses of the OA-Related Targets

GO and KEGG pathway enrichment studies have elucidated the various roles of the OA-related targets (Table S6). 495 proteins were used to build the OA PPI network, then 9 clusters were established by the MCODE algorithm (Figure 4A and B). The KEGG pathway analysis was applied separately to each MCODE, and the three best-scoring p-value terms were preserved as the usable explanation of the corresponding MCODE (Table 2). GO analysis consists of three items: BP, CC, and MF, which is shown in Figure 4C–E. In the BP analysis (Figure 4C), response to toxic substance (GO:0009636) had the highest value, indicating that OA was most sensitive to toxic substance. Furthermore, response to oxidative stress (GO:0006979), response to oxygen levels (GO:0070482), and reactive oxygen species metabolic process (GO:0072593) show that oxidative stress (OS) is a vital event in the pathogenesis of OA. Aging (GO:0007568), developmental process involved in reproduction (GO:0003006), gland development (GO:0048732), and response to growth factor (GO:0070848) suggest that growth and development in human body play crucial role in the pathogenesis process of OA. Apoptotic signaling pathway (GO:0097190), and positive regulation of cell death (GO:0010942) are also important. Response to steroid hormone (GO:0048545), and steroid metabolic process (GO:0008202) are the essential mechanism in OA pathogenesis. In the CC section (Figure 4D), sperm part (GO:0097223) has the direct association with OA. Cyclin-dependent protein kinase holoenzyme complex (GO:0000307) is related to apoptosis. Peroxisome (GO:0005777) correlates directly to oxidant stress. In the analysis of MF (Figure 4E), The p-value of oxidoreductase

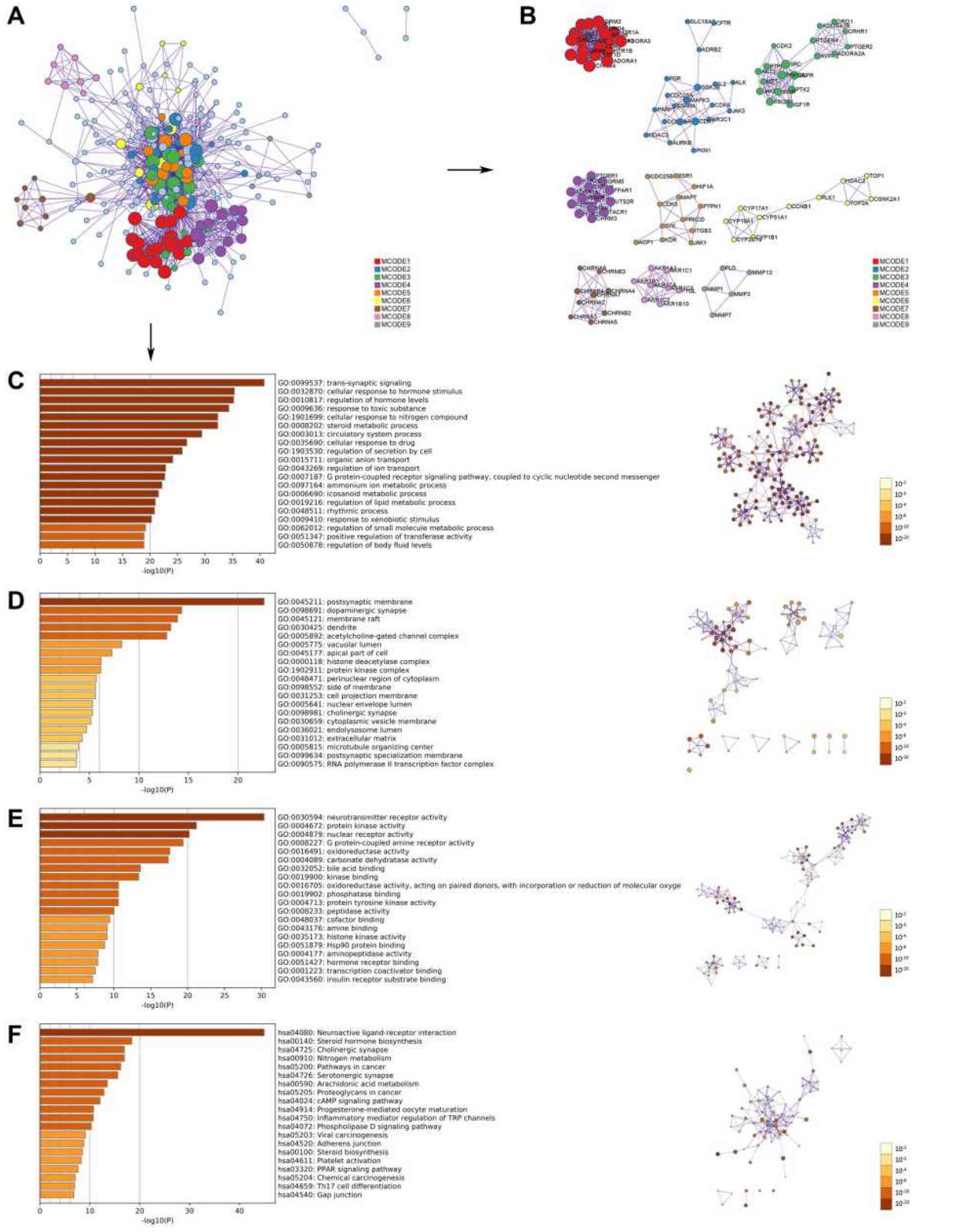

Figure 2 GO and KEGG pathway enrichment analyses of the CSMFCH component-target network (p-value ≤ 0.05). (**A**) The PPI network. (**B**) The clusters of PPI network. The colors indicate diverse clusters or binding site sets that are predicted by the MCODE algorithm. (**C**) The top 20 biological processes. (**D**) The top 20 cellular components. (**E**) The top 20 molecular functions. (**F**) The top 20 KEGG pathways. The bar plot and different colors show the enrichment scores [-log10 (P-value)] of the top 20 significant enrichments.

Abbreviations: GO, Gene Ontology; KEGG, Kyoto Encyclopedia of Genes and Genomes; CSMFCH,*Cuscutae Semen-Mori Fructus* coupled-herbs; PPI, protein–protein interaction.

Table 1 Three Best-Scoring Terms of KEGG Pathway Analysis Applied to Each MCODE of the CSMFCH Component-Target Network

MCODE	KEGG	Description	Log10(P)
MCODE 1	hsa04080 hsa04024 hsa04072	Neuroactive ligand-receptor interaction cAMP signaling pathway Phospholipase D signaling pathway	−30.2 −8 −7
MCODE 2	hsa04914 hsa04110 hsa04114	Progesterone-mediated oocyte maturation Cell cycle Oocyte meiosis	−7.9 −7.3 −7.3
MCODE 3	hsa04015 hsa01521 hsa05205	Rap1 signaling pathway EGFR tyrosine kinase inhibitor resistance Proteoglycans in cancer	−15.8 −15.2 −13.9
MCODE 4	hsa04080 hsa04020 hsa04810	Neuroactive ligand-receptor interaction Calcium signaling pathway Regulation of actin cytoskeleton	−24.3 −21 −5.3
MCODE 5	hsa05205 hsa04151 hsa04919	Proteoglycans in cancer PI3K-Akt signaling pathway Thyroid hormone signaling pathway	−5.7 −4.8 −4.6
MCODE 6	hsa04913 hsa00140 hsa04110	Ovarian steroidogenesis Steroid hormone biosynthesis Cell cycle	−5.9 −5.7 −4.7
MCODE 7	hsa04080 hsa04725 hsa05033	Neuroactive ligand-receptor interaction Cholinergic synapse Nicotine addiction	−17.6 −12.2 −9.1
MCODE 8	hsa00140 hsa00040 hsa00561	Steroid hormone biosynthesis Pentose and glucuronate interconversions Glycerolipid metabolism	−8.7 −6.9 −6.1
MCODE 9	hsa04657	IL-17 signaling pathway	−6.3

Abbreviations: KEGG, Kyoto Encyclopedia of Genes and Genomes; MCODE, Multi Contrast Delayed Enhancement; CSMFCH, *Cuscutae Semen-Mori Fructus* coupled-herbs.

activity (GO:0016491), and antioxidant activity (GO:0016209) is high, again illustrating the importance of OS in OA pathogenesis. For the KEGG pathway enrichment analysis (Figure 4F), our results showed that OA is associated with cancer, such as Pathways in cancer (hsa05200), MicroRNAs in cancer (hsa05206), Transcriptional misregulation in cancer (hsa05202). In addition, Apoptosis (hsa04210), HIF-1 signaling pathway (hsa04066), Estrogen signaling pathway (hsa04915) correspond to apoptosis, OS, and hormone regulation processes. We also found that virus and bacteria are the non-negligible reason inducing OA, including HTLV-I infection (hsa05166), Epstein-Barr virus infection (hsa05169), and Legionellosis (hsa05134). Therefore, OS, hormone diagnosis, apoptosis, invasion of virus and bacteria, and cancer, constitute the main causes of OA. The result of Table 2 also confirmed it.

CSMFCH-OA Common-Target Network

Taking the intersection of the OA-related targets and CSMFCH targets, we obtained 64 CSMFCH-OA common targets (Figure 5A). Next, we constructed the CSMFCH-OA common target network (Figure 5B). These targets come from 13 bioactive components of CS, 6 bioactive components of MF, and 3 common components of CS and MF. The degree value of the CSMFCH-OA common-target network was calculated to screen the core bioactive components and related targets (Table S8). The result shows that kaempferol is the most significant component from CS and MF, which would be further explored below. Quercetin and beta-sitosterol also play a very important role in the CSMFCH-OA common-target network. Additionally, the top 10 degree values of these genes in the network are aromatase (CYP19A1), estrogen receptor beta (ESR2), cholinesterase (BCHE), androgen receptor

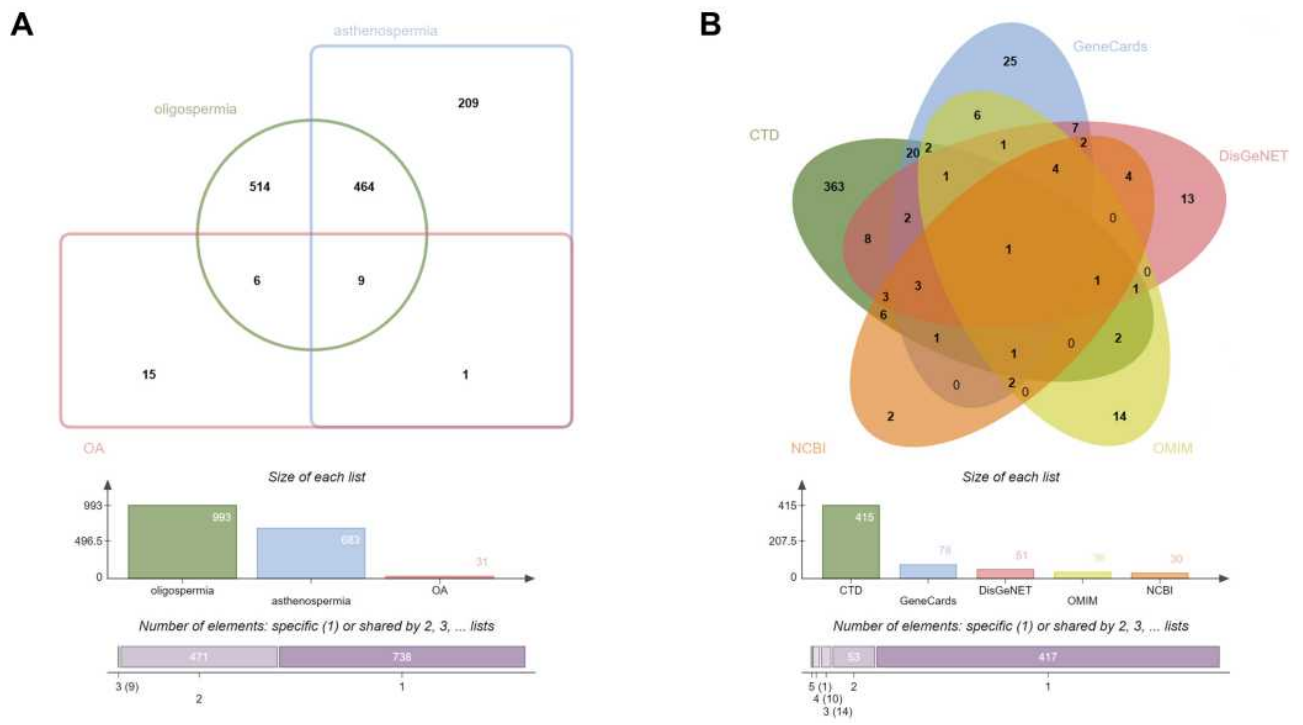

Figure 3 OA-related targets. (**A**) Venn diagram: OA-related targets are 495, including 473 common targets between oligospermia and asthenozoospermia, and 31 targets from the search term "oligoasthenozoospermia". (**B**) Venn diagram: the number of OA-related targets from the five different databases is 415, 78, 51, 36, and 30, respectively. The common target is androgen receptor (AR).
Abbreviations: OA, oligoasthenozoospermia; AR, androgen receptor.

(AR), acetylcholinesterase (ACHE), estrogen receptor (ESR1), 3-hydroxy-3-methylglutaryl-coenzyme A reductase (HMGCR), oxysterols receptor LXR-alpha (NR1H3), steroid 17-alpha-hydroxylase/17, 20 lyase (CYP17A1), Poly [ADP-ribose] polymerase 1 (PARP1).

The PPI Network and Cluster Analysis

To classify the PPI information, a total of 64 CSMFCH-OA common targets have been submitted to the STRING database (Figure 6A). Then, we used the Cytoscape software to generate the PPI network, which comprised 64 nodes and 426 edges (Figure 6B). To identify the hub nodes and essential proteins in the PPI network, the topological parameters of the nodes were calculated by Network Analyzer, including seven centralities (average shortest path length, betweenness, centrality, closeness centrality, clustering coefficient, degree, and combined score) (Table S9). Depending on the degree value and combined score of the network topology analysis, the top 10 proteins were RAC-alpha serine/threonine-protein kinase (AKT1), epidermal growth factor receptor (EGFR), mitogen-activated protein kinase 3 (MAPK3), estrogen receptor (ESR1), prostaglandin G/H synthase 2 (PTGS2), androgen receptor (AR), matrix metalloproteinase-9 (MMP9), progesterone receptor (PGR), Peroxisome proliferator-activated receptor gamma (PPARG), aromatase (CYP19A1). In addition, with a view to understanding the underlying mechanism of CSMFCH against OA, the PPI network was divided into 4 clusters (Figure 6C–F). Next, the PPI network and 4 clusters were profoundly enriched by GO and KEGG.

GO and KEGG Pathway Enrichment Analyses of the PPI Network

The most enriched 20 GO terms were acquired from Figure 7, with a total of 64 proteins primarily included in GO and KEGG pathway enrichment (Table S11). The BP was related to response to oxidative stress (GO:0006979), reactive oxygen species metabolic process (GO:0072593), cellular response to oxidative stress (GO:0034599), regulation of reactive oxygen species metabolic process (GO:2000377), cellular response to reactive oxygen species (GO:0034614), indicating that CSMFCH has an antioxidant effect on OA (Figure 7A). Moreover, response to steroid hormone (GO:0048545), response to peptide

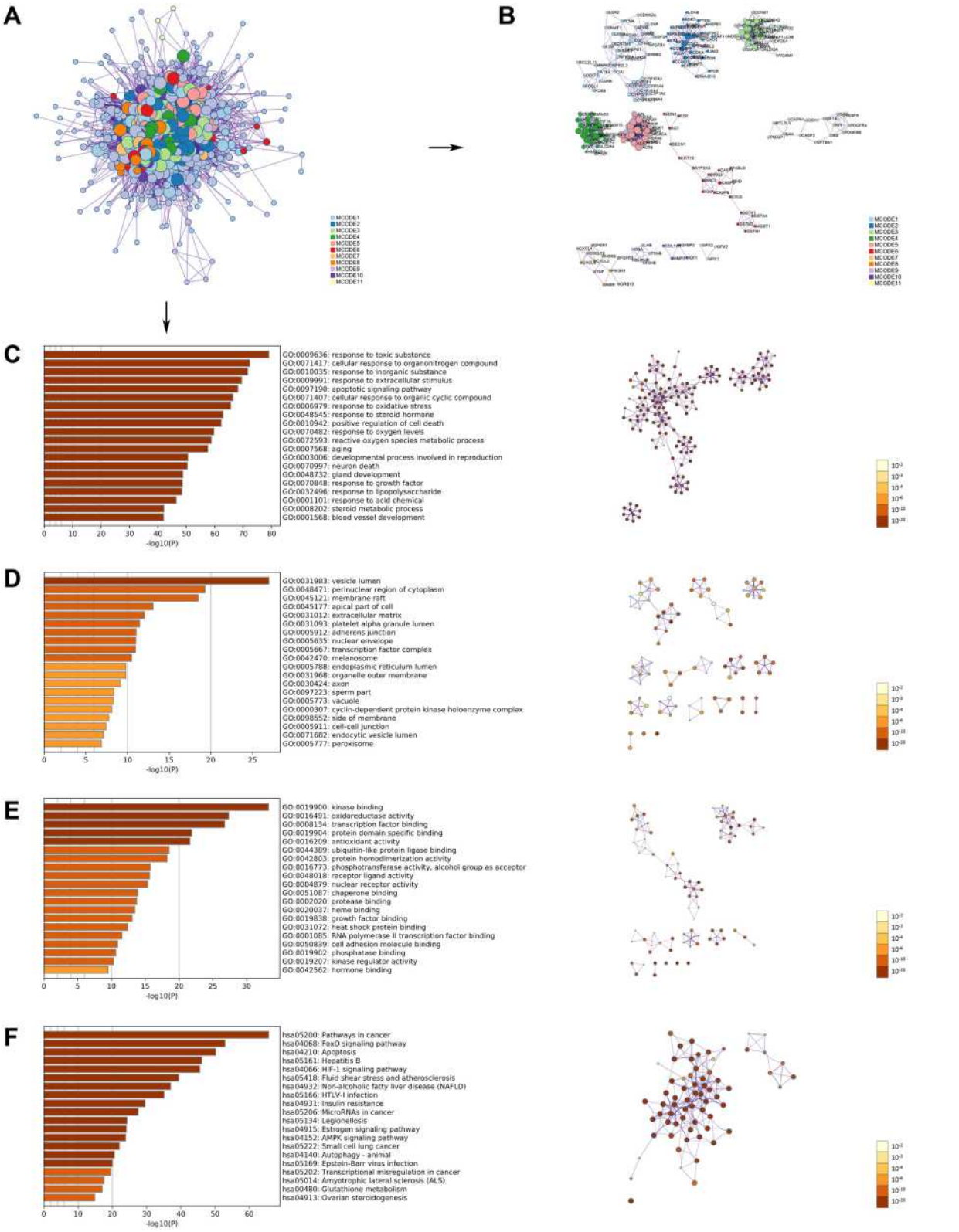

Figure 4 GO and KEGG pathway enrichment analyses of the OA-related targets (p-value ≤ 0.05). (**A**) The PPI network. (**B**) The clusters of PPI network. The colors represent different clusters or sets of binding sites predicted by MCODE algorithm. (**C**) The top 20 biological processes. (**D**) The top 20 cellular components. (**E**) The top 20 molecular functions. (**F**) The top 20 KEGG pathways. The bar plot and different colors show the enrichment scores [-log10 (P-value)] of the top 20 significant enrichments.

Abbreviations: GO, Gene Ontology; KEGG, Kyoto Encyclopedia of Genes and Genomes; OA, oligoasthenozoospermia; PPI, protein–protein interaction.

Table 2 Three Best-Scoring Terms of KEGG Pathway Analysis Applied to Each MCODE of the OA-Related Targets

MCODE	KEGG	Description	Log10(P)
MCODE 1	hsa00140 hsa04210 hsa04913	Steroid hormone biosynthesis Apoptosis Ovarian steroidogenesis	−13.3 −10.2 −9.7
MCODE 2	hsa04151 hsa05215 hsa05200	PI3K-Akt signaling pathway Prostate cancer Pathways in cancer	−17.2 −16.8 −14.7
MCODE 3	hsa04068 hsa05200 hsa05161	FoxO signaling pathway Pathways in cancer Hepatitis B	−25.6 −21.9 −18.6
MCODE 4	hsa05200 hsa05215 hsa04915	Pathways in cancer Prostate cancer Estrogen signaling pathway	−13.2 −11.6 −11.2
MCODE 5	hsa01200 hsa00010 hsa_M00001	Carbon metabolism Glycolysis/Gluconeogenesis Glycolysis (Embden-Meyerhof pathway), glucose ≤ pyruvate	−12.9 −8.3 −8
MCODE 6	hsa01524 hsa04215 hsa04210	Platinum drug resistance Apoptosis - multiple species Apoptosis	−25.6 −18.3 −13
MCODE 7	hsa05200 hsa01521 hsa04015	Pathways in cancer EGFR tyrosine kinase inhibitor resistance Rap1 signaling pathway	−12.9 −11.6 −11
MCODE 8	hsa05134 hsa04062 hsa05323	Legionellosis Chemokine signaling pathway Rheumatoid arthritis	−8.1 −8 −7.2
MCODE 9	hsa04080 hsa04913 hsa04912	Neuroactive ligand-receptor interaction Ovarian steroidogenesis GnRH signaling pathway	−9.7 −7.1 −6.3
MCODE 11	hsa00480 hsa00590 hsa04918	Glutathione metabolism Arachidonic acid metabolism Thyroid hormone synthesis	−8 −7.8 −7.6

Abbreviations: KEGG, Kyoto Encyclopedia of Genes and Genomes; MCODE, Multi Contrast Delayed Enhancement; OA, oligoasthenozoospermia.

hormone (GO:0043434), cellular response to steroid hormone stimulus (GO:0071383), and hormone biosynthetic process (GO:0042446) show that CSMFCH could regulate hormone in the pathogenesis of OA. The CC was associated with membrane raft (GO:0045121), membrane microdomain (GO:0098857) and membrane region (GO:0098589), demonstrating that CSMFCH acts on cell membrane in cellular (Figure 7B). The MF was relevant to steroid hormone receptor activity (GO:0003707), and hormone binding (GO:0042562), revealing that the importance of hormone on OA (Figure 7C). Oxidoreductase activity, acting on paired donors, with incorporation or reduction of molecular oxygen (GO:0016705), oxidoreductase activity, acting on the CH-OH group of donors, NAD or NADP as acceptor (GO:0016616), oxidoreductase activity, acting on CH-OH group of donors (GO:0016614), and oxygen binding (GO:0019825) in MF indicate CSMFCH decreases OS against OA. A total of 117 KEGG pathways were enriched, and the top 20 enriched pathways were shown in Figure 7D. According to the above results, we assume that CSMFCH might treat OA by regulating the endocrine and hormones process through Prolactin signaling pathway (hsa04917), Endocrine resistance (hsa01522), Estrogen signaling pathway (hsa04915),

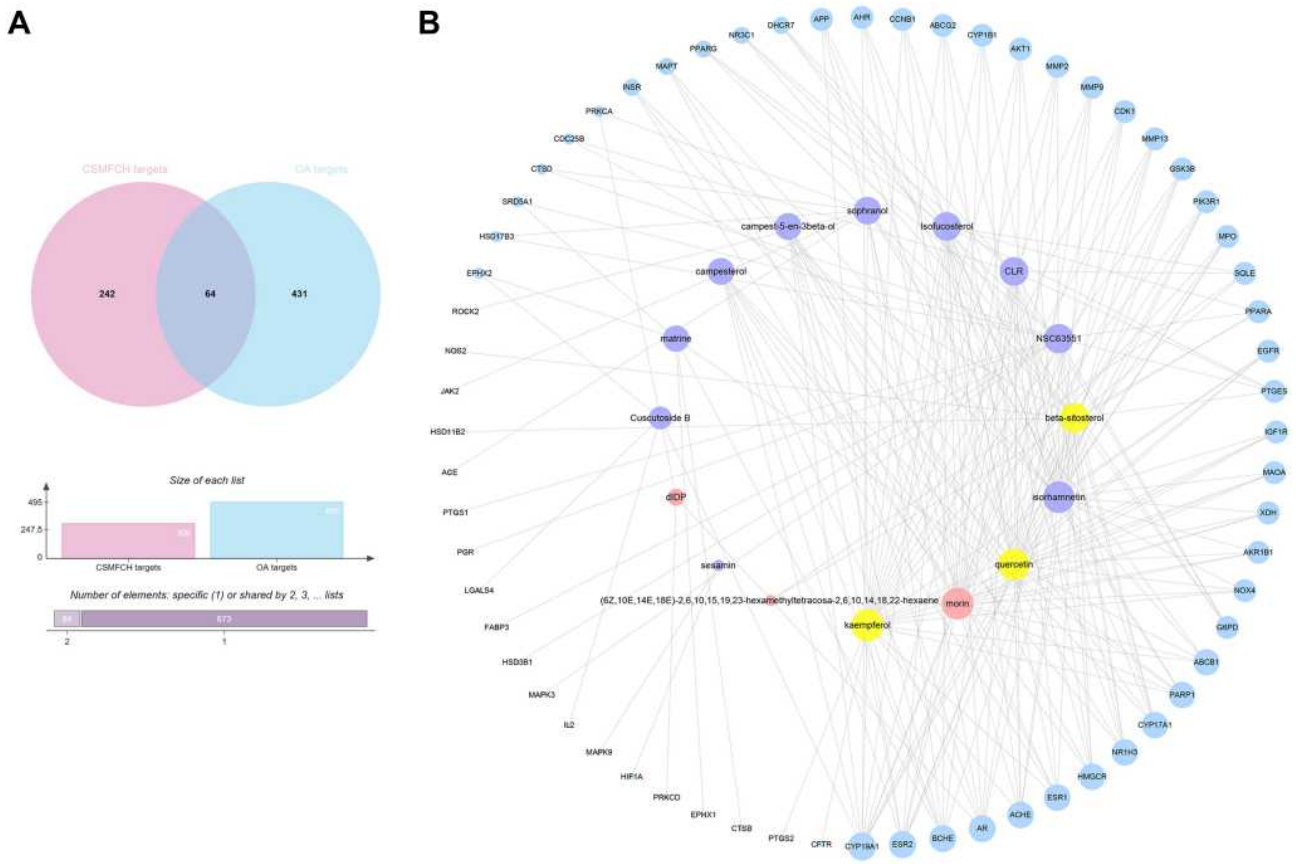

Figure 5 CSMFCH-OA common-target network. (**A**) Intersection of Venn diagram: 64 targets are common to CSMFCH and OA. (**B**) Common-target network, including 80 nodes and 218 edges. The size of the circle represents the node degree of the target protein. Purple nodes and pink nodes stand for bioactive components from CS and MF, respectively. Yellow node stands for the common components from CS and MF. Blue nodes stand for targets.
Abbreviations: CSMFCH,*Cuscutae Semen-Mori Fructus* coupled-herbs; OA, oligoasthenozoospermia; CS, *Cuscutae Semen*; MF, *Mori Fructus*.

Relaxin signaling pathway (hsa04926), Steroid hormone biosynthesis (hsa00140). CSMFCH also decreases OS by means of AGE-RAGE signaling pathway in diabetic complications (hsa04933), and HIF-1 signaling pathway (hsa04066). GlueGO was used to further investigate the enrichment of GO and KEGG, revealing that decreasing OS and regulating hormones play a key role in promoting male reproductive function against OA (Figure 7E–H).

GO and KEGG Pathway Enrichment Analyses of the Clusters

Analyses of GO and KEGG pathway enrichment were applied to measure the clusters (Figure 8). The GO and KEGG pathway enrichment result reveals that the proteins in cluster 1 are mostly related to the production of reproductive structure and system and hormone modulation pathways, just like the findings of the PPI network analysis (Figure 8A and B). In addition, the proteins of cluster 2 correlate to OS, and hormone regulation pathways (Figure 8C and D). Besides, the result of cluster 3 shows that CSMFCH could treat OA by improving androgen biosynthetic process, and male genitalia development (Figure 8E and F). The outcomes of cluster 4 indicate that MOLOCH also enhances the capability of vascular endothelial growth factor in the anti-OA system (Figure 8G and H). Therefore, we further conclude that CSMFCH's mechanism against OA is hormone regulation, OS reduction, and male reproductive function promotion through the GO and KEGG pathway enrichment analyses of the clusters.

Core Component-Target-Pathway Network

The core component-target-pathway network was developed by Cytoscape software, in order to explore CSMFCH's molecular mechanism against OA in detail. A total of 75 nodes and 295 edges were estimated, shown

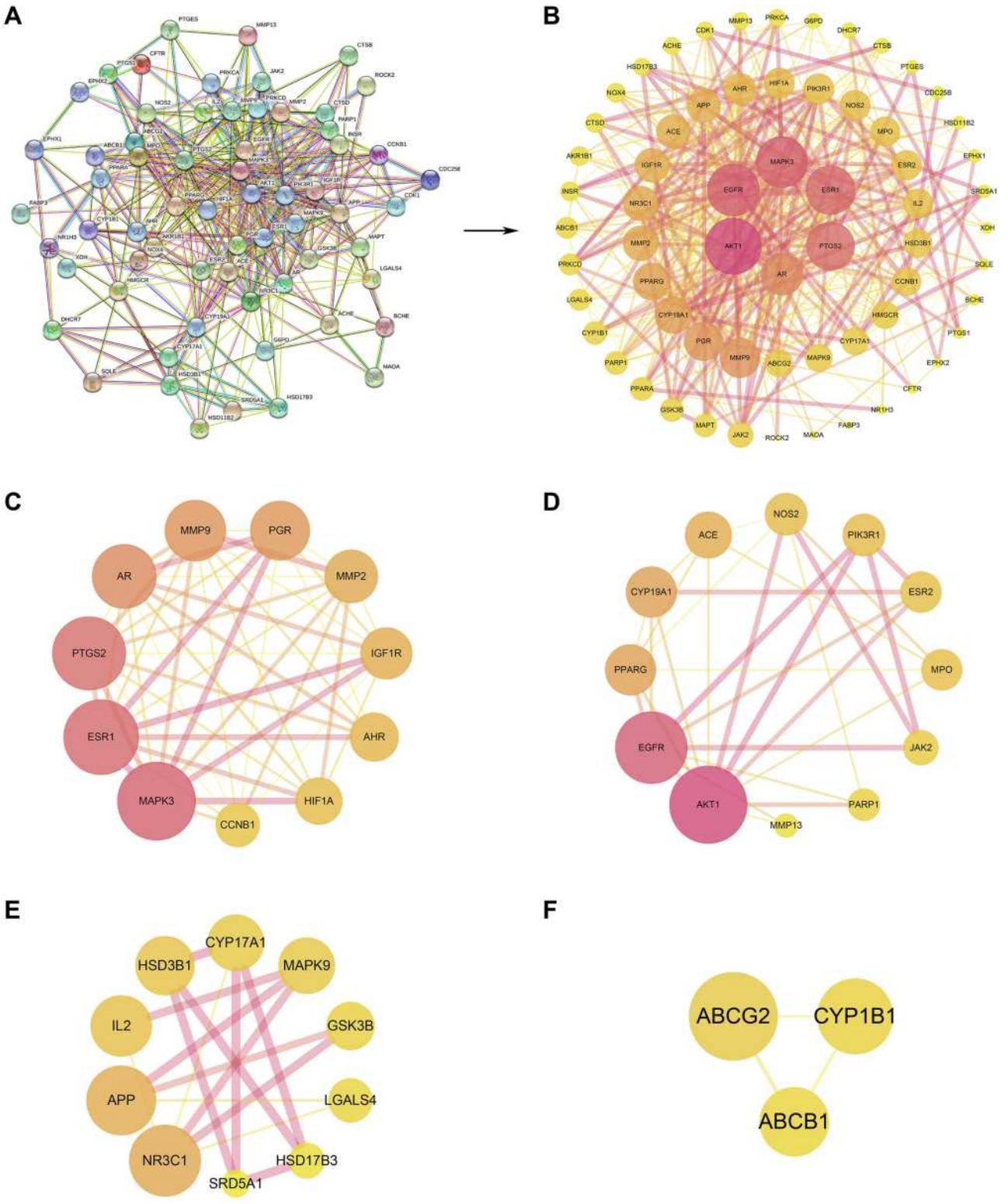

Figure 6 The PPI network and cluster analysis. (**A**) The PPI information generated by the STRING database. (**B**) The PPI network visualized using the Cytoscape software. (**C**) Cluster 1 (score = 9.6). (**D**) Cluster 2 (score = 5.455). (**E**) Cluster 3 (score = 3.333). (**F**) Cluster 4 (score = 3). The size and color of the node represent the degree of the target protein. The width and color of the edge represent the combined score of the target protein.
Abbreviation: PPI, protein–protein interaction.

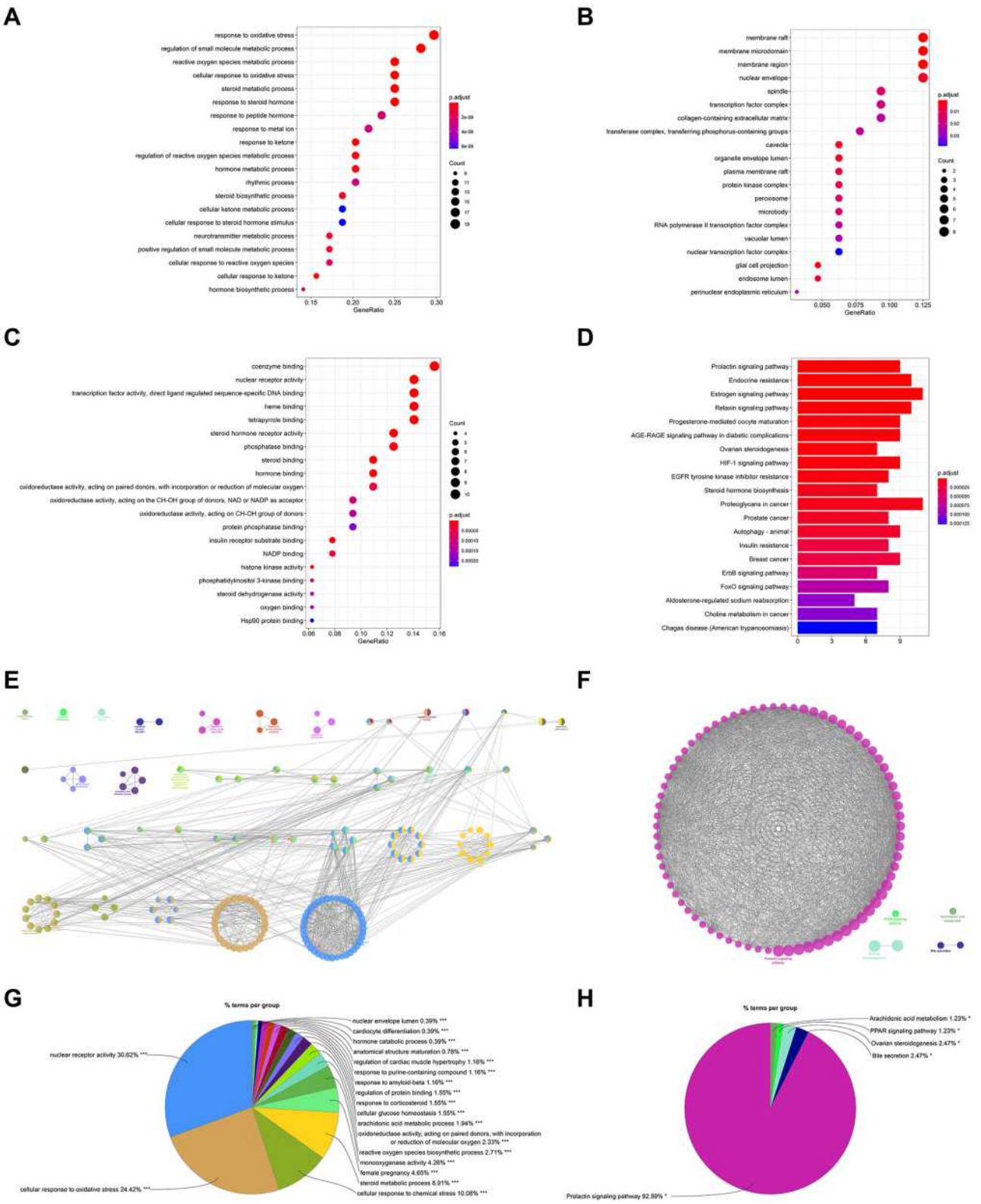

Figure 7 GO and KEGG pathway enrichment analyses of the PPI network (p-value ≤ 0.05). (**A**) The top 20 biological processes. (**B**) The top 20 cellular components. (**C**) The top 20 molecular functions. (**D**) The top 20 KEGG pathways. The color scales indicate the different thresholds for the p-values. (**E** and **G**) The GO enrichment of the PPI network using the ClueGo plugin. Show only pathways with ***P≤0.001. (**F** and **H**) The KEGG pathway analysis of the PPI network using the ClueGo plugin. Show only pathways with *P≤0.05.

Abbreviations: GO, Gene Ontology; KEGG, Kyoto Encyclopedia of Genes and Genomes; PPI, protein–protein interaction.

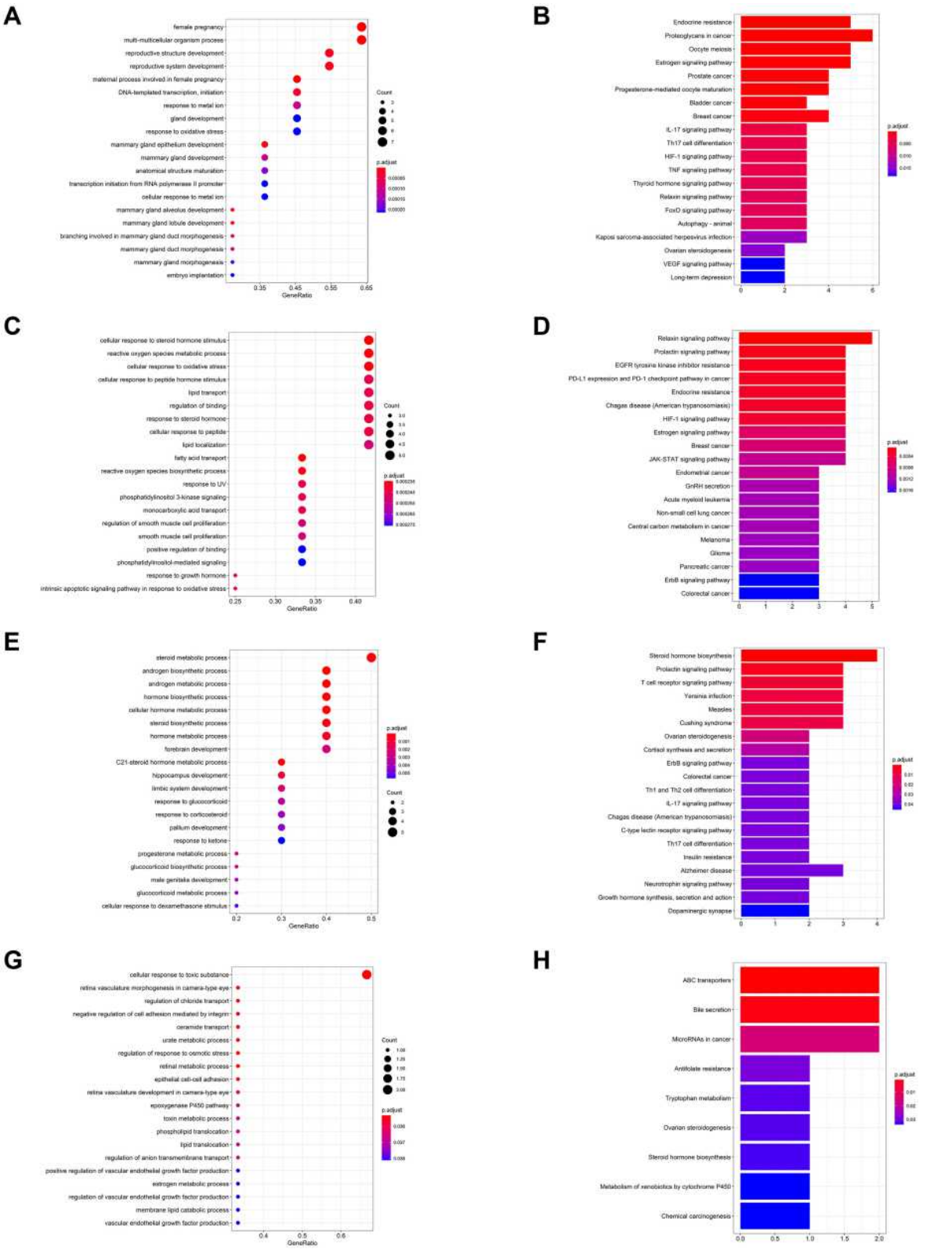

Figure 8 GO and KEGG pathway enrichment analyses of the clusters (p-value ≤ 0.05). (**A**) The top 20 biological processes for cluster 1. (**B**) The top 20 KEGG pathways for cluster 1. (**C**) The top 20 biological processes for cluster 2. (**D**) The top 20 KEGG pathways for cluster 2. (**E**) The top 20 biological processes for cluster 3. (**F**) The top 20 KEGG pathways for cluster 3. (**G**) The top 20 biological processes for cluster 4. (**H**) Nine KEGG pathways for cluster 4. The color scales indicate the different thresholds for the p-values.

Abbreviations: GO, Gene Ontology; KEGG, Kyoto Encyclopedia of Genes and Genomes.

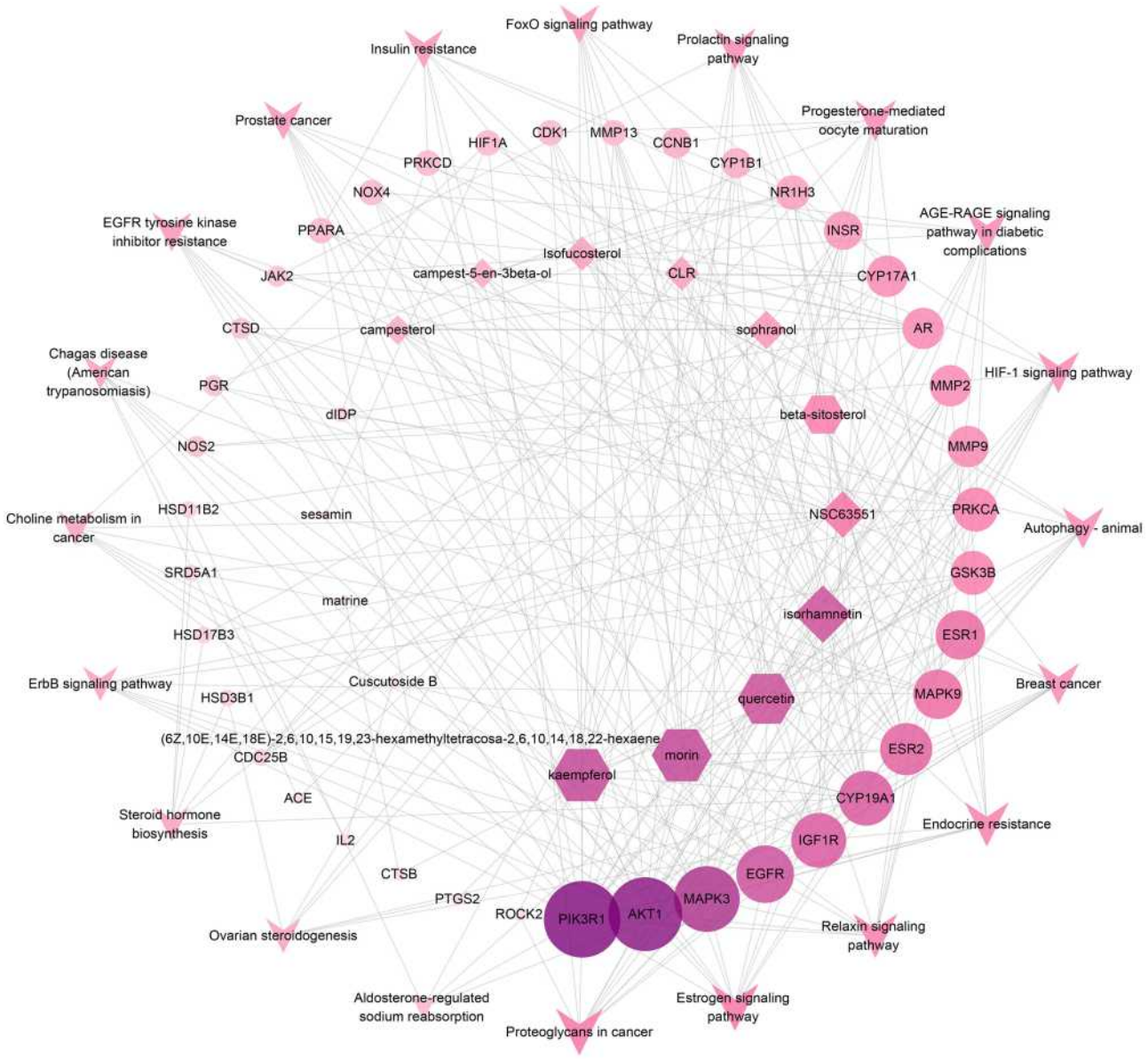

Figure 9 Core component-target-pathway network. The V nodes represent the top 20 KEGG signaling pathways. The ellipse nodes represent the targets related to the pathways. The diamond nodes represent ingredients from CS, and the hexagon nodes represent ingredients from MF. The size of the circle represents the node degree of the target protein.

Abbreviations: KEGG, Kyoto Encyclopedia of Genes and Genomes; CS, *Cuscutae Semen*; MF, *Mori Fructus*.

in Figures 9 and 16 bioactive components were found. According to the degree value obtained from Network Analyzer, the most remarkable component is kaempferol (Figure 10). We selected 20 terms as the major signaling pathways basis on the findings of GO and KEGG pathway enrichment analyses of the PPI network. Among these, the most significant pathway is estrogen signaling pathway (Figure 11). The top 10 genes are Phosphatidylinositol 3-kinase regulatory subunit alpha (PIK3R1), RAC-alpha serine/threonine-protein kinase (AKT1), Mitogen-activated protein kinase 3 (MAPK3), Epidermal growth factor receptor (EGFR), Insulin-like growth factor 1 receptor (IGF1R), Aromatase (CYP19A1), Estrogen receptor beta (ESR2), Mitogen-activated protein kinase 9 (MAPK9), Estrogen receptor (ESR1), Glycogen synthase kinase-3 beta (GSK3B).

Molecular Docking

Molecular docking is a tool for predicting how a protein interacts with small molecules (ligands) using molecular

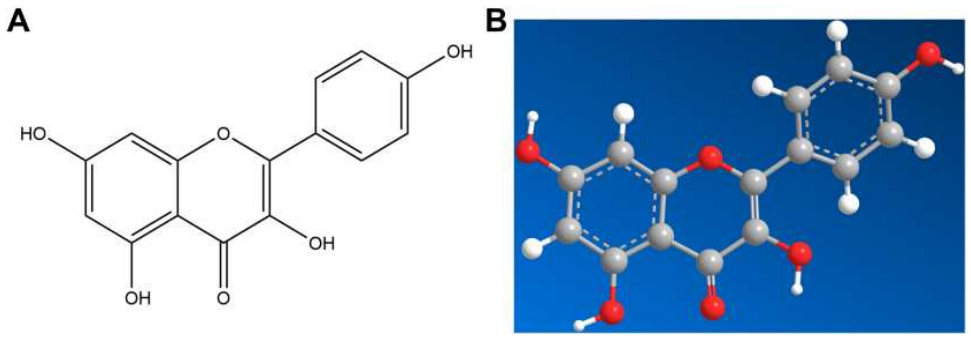

Figure 10 The molecular structure of kaempferol was shown as 2D diagrams (**A**) and 3D diagrams (**B**).

computational methods.[78] According to the above results, we thought Kaempferol is the most significant component of CSMFCH against OA. AKT1, EGFR, MAPK3, ESR1, CYP19A1 are the overlapping targets between the top 10 targets of the PPI network and the core component-targets-pathway network. In addition, AR is the only common target from five different databases. In order to further investigate the interactions between core components and key targets of CSMFCH in treating OA, we chose kaempferol as the small molecule (ligand), AKT1, EGFR, MAPK3, ESR1, CYP19A1, and AR as proteins to perform the molecular docking. The obtained docking results

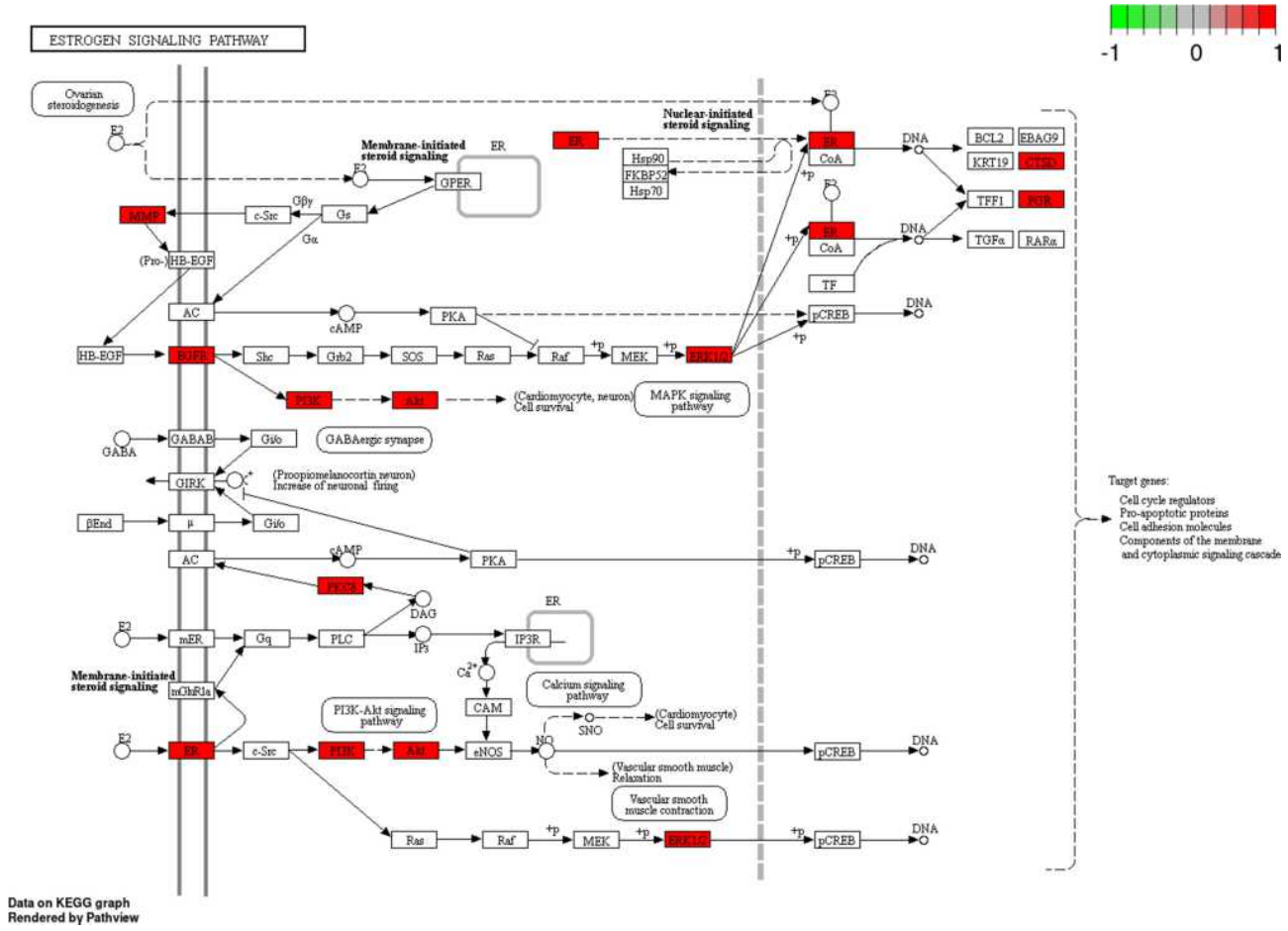

Figure 11 Estrogen signaling pathway. The red rectangle represents the targets related to the PPI network.
Abbreviation: PPI, protein–protein interaction.

indicated that the receptor-ligand interaction between drugs and proteins includes hydrophobic interactions and polar interactions. According to Table 3, AKT1, EGFR, MAPK3, ESR1, CYP19A1, and AR have strong binding interactions with kaempferol.

Kaempferol was docked with seven residues to form hydrophobic interactions in AKT1 (Asp274, Gly294, Ser7, Lys179, Leu181, Gly162, and Gly159) and 4 hydrogen bonds (kaempferol$_{O5}$: Asp292$_{o}$ (2.9 Å) and Leu295$_{N}$, (2.8 Å), kaempferol$_{O4}$: Phe161$_{N}$ (3.1 Å) and Thr160$_{N}$, (2.8 Å)) (Figure 12A and B). In addition, kaempferol was predicted to interact with EGFR via Ala743, Leu792, Leu718, Cys797, Arg841, Leu844, Gly796 and form 3 hydrogen bonds with the residue Met793 (3.0 Å), Asn842 (2.8 Å), Asp855 (2.9 Å) (Figure 12C and D). Kaempferol could bind to MAPK3 by forming hydrophobic interactions with the neighboring residues Gly262, Lys 287, Gly259, Asn255, Leu284, Leu258 and two hydrogen bonds with Ser263 (3.0 Å), and Pro285 (3.2 Å) (Figure 12E and F). Besides, kaempferol bound to a pocket in ESR1, which was composed of Ala350, Leu391, Leu387, Leu384, Leu525, Met421, Ile424, andGly521. 3 hydrogen bonds formed by kaempferol$_{O5}$: Arg394$_{NH2}$ (3.0 Å) and Glu353$_{OE1}$ (2.8 Å), and kaempferol$_{O4}$: His524$_{ND1}$ (3.3 Å) further enhanced the interaction between the ligand and the ESR1 protein (Figure 12G and H). Furthermore, kaempferol was docked to CYP19A1 by forming hydrophobic interactions with the neighboring residues (Arg115, Cys437, Arg145, Ile133, Ile132, Ala306, Gly439, Gly436, Leu152, Ala438) and 3 hydrogen bonds with Arg435 (2.9 Å), Trp1 (3.3 Å), and Thr310 (2.7 Å) (Figure 12I and J). Kaempferol binds to AR by forming hydrophobic interactions with the neighboring residues Gln711, Met749, Val746, Leu873, Met780, Phe876, Met895, Gly708, Leu707 and 5 hydrogen bonds with Arg752 (2.8 Å), Met745 (2.8 Å), Leu704 (2.7 Å), Asn705 (2.6 Å), and Thr877 (2.8 Å) (Figure 12K and L).

Table 3 Results of Molecular Docking Between Kaempferol and the Predicted Targets

Ligand	Proteins	Affinity (kcal/mol)	Dist from Best Mode	
			rmsd l.b.	rmsd u.b.
Kaempferol	AKT1	−7.5	0.000	0.000
	EGFR	−6.6	0.000	0.000
	MAPK3	−5.4	0.000	0.000
	ESR1	−7.4	0.000	0.000
	CYP19A1	−7.3	0.000	0.000
	AR	−8.4	0.000	0.000

UHPLC-Q-Orbitrap-MS Analysis

Q-Exactive orbitrap mass spectrometer was used to analyze the active components of CSMFCH. The element compositions of kaempferol and MS2 fragment ions were calculated by their accurate mass measurements. The retention times, molecular formulas, high-resolution MS data and high resolution MS2 fragment ions in negative and positive modes are shown in Figures 13 and 14, respectively. As shown in Figures 13B and 14B, kaempferol was identified by Compound discover software and PubChem database, which validated the consistency of our network pharmacology results.

The Viability of TM3 and TM4 Cells in the Treatment of CSMFCH and Kaempferol

After CSMFCH treatment, the absorbance of TM3 cells increased significantly compared with the non-treatment group (all $P < 0.01$) (Figure 15A). In addition, the cell viability of TM3 cells was enhanced to above 125% (Figure 15B). Treatment with high dose of kaempferol (1 μg/mL $p < 0.01$, 0.5 μg/mL $P < 0.05$ and 0.25 μg/mL $P < 0.05$) could improve the absorbance and cell viability in TM3 cells (Figure 15C and D). Similarly, the absorbance and activity of TM4 cells were elevated by CSMFCH ($P < 0.05$), except for the lowest dosage (0.007813 mg/mL) (Figure 5E and F). As shown in Figure 15G and H, the absorbance and cell activity of TM4 cells in the treatment of kaempferol were significantly boosted compared with that of control cells (all $P < 0.01$). These results indicated that CSMFCH and kaempferol could both improve the viability of TM3 and TM4 cells. This validated the network pharmacology results described above.

The Body, Testicular, and Epididymal Weight of OA Mice in the Treatment of CSMFCH and Kaempferol

Compared with the NC group, CP significantly decreased the body, testicular, and epididymal weight in the MC group (all $P < 0.01$). The kaempferol group and low-, medium-, and high-dose CSMFCH groups significantly improved the body, testicular, and epididymal weight compared with the MC group (all $P < 0.05$). The results are presented in Figure 16.

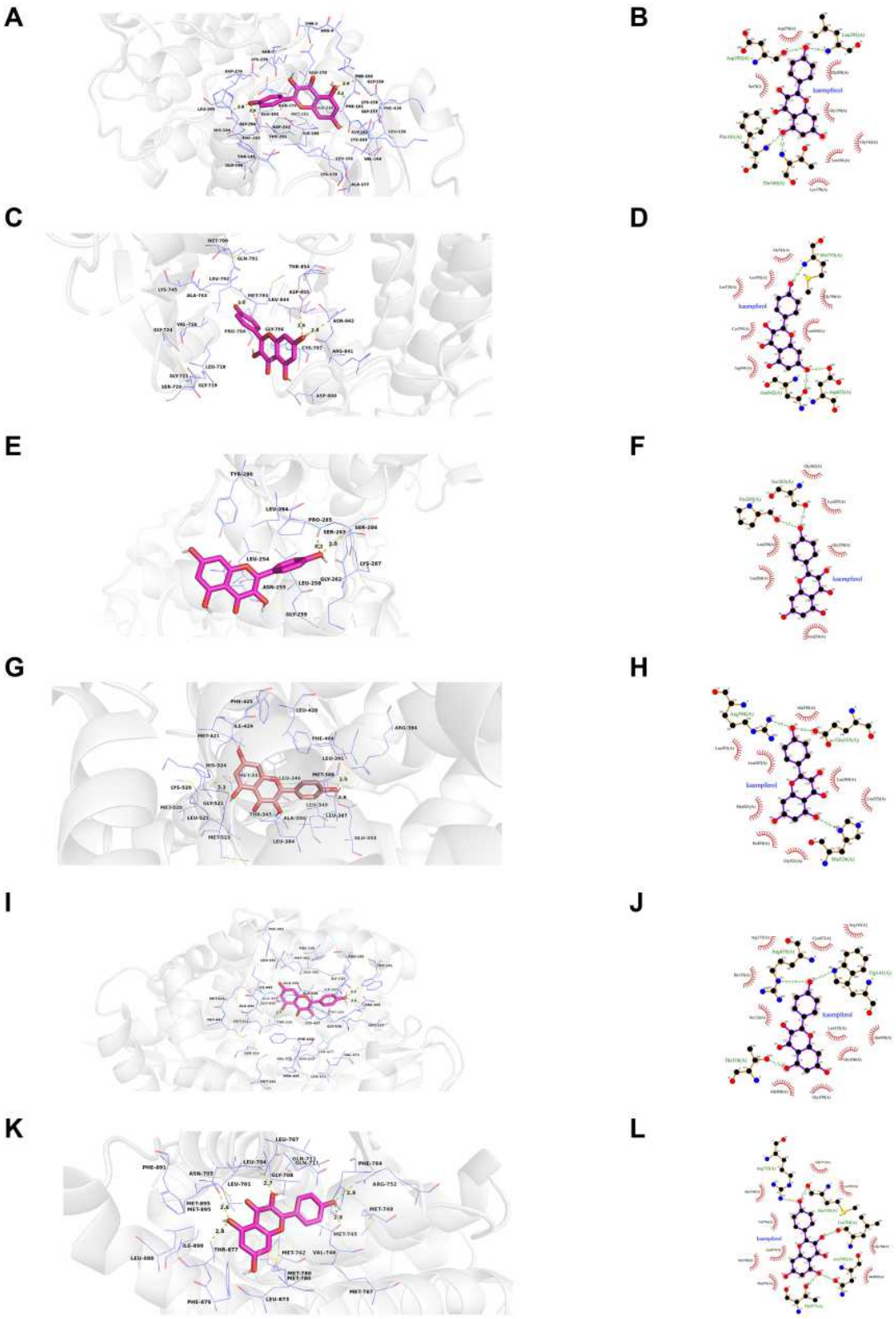

Figure 12 Molecular models of the binding of kaempferol from CSMFCH to the predicted targets (**A** and **B**) AKT1, (**C** and **D**) EGFR, (**E** and **F**) MAPK3, (**G** and **H**) ESR1, (**I** and **J**) CYP19A1, and (**K** and **L**) AR shown as 3D diagrams and 2D diagrams.

Abbreviations: AKT1, RAC-alpha serine/threonine-protein kinase; EGFR, epidermal growth factor receptor; MAPK3, mitogen-activated protein kinase 3; ESR1, estrogen receptor; CYP19A1, aromatase; AR, androgen receptor.

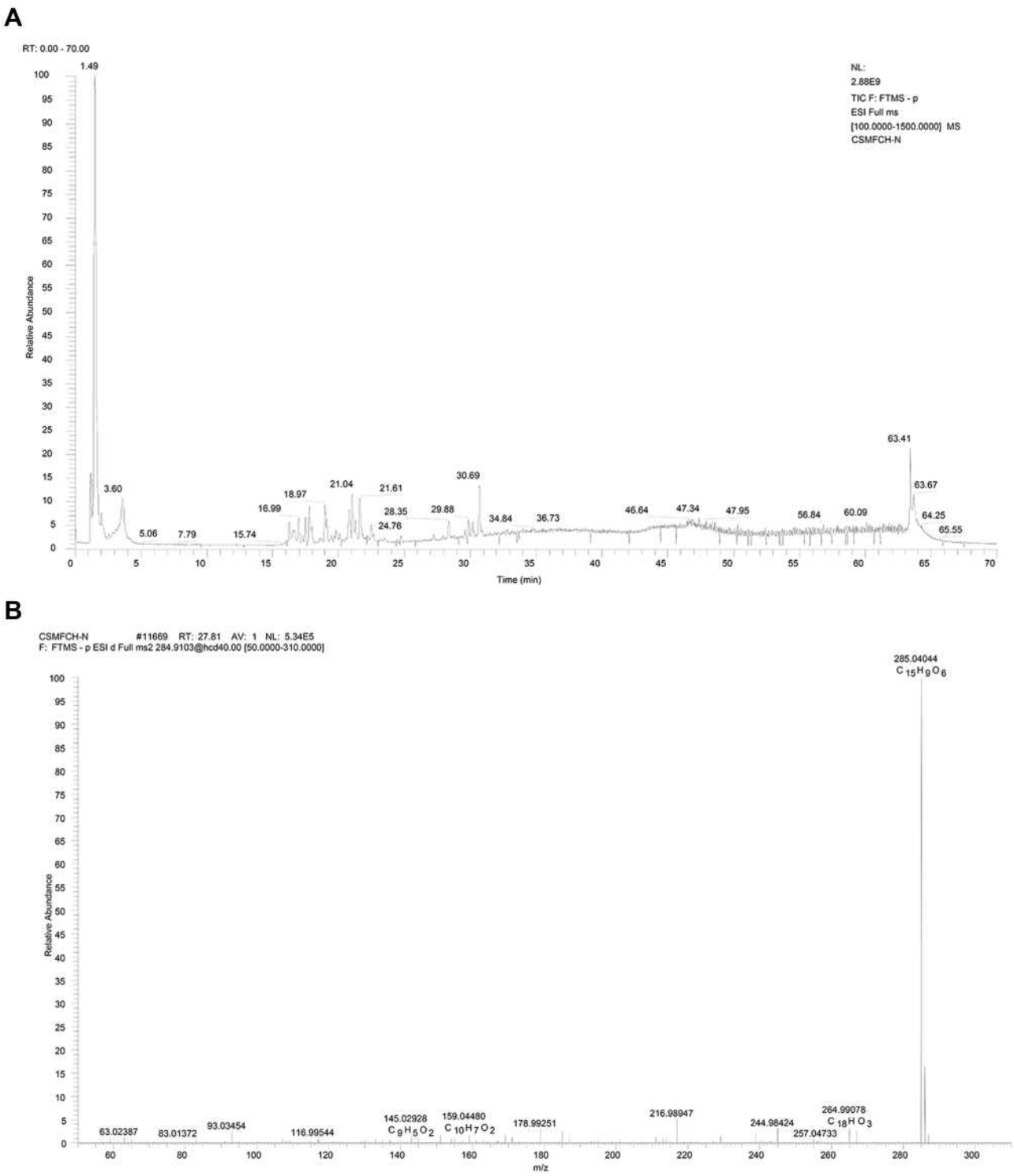

Figure 13 Mass spectrum of CSMFCH in the negative ion mode. (**A**) Total ion current chromatogram of CSMFCH. (**B**) ESI-MS/MS spectra of kaempferol.
Abbreviation: CSMFCH,*Cuscutae Semen-Mori Fructus* coupled-herbs.

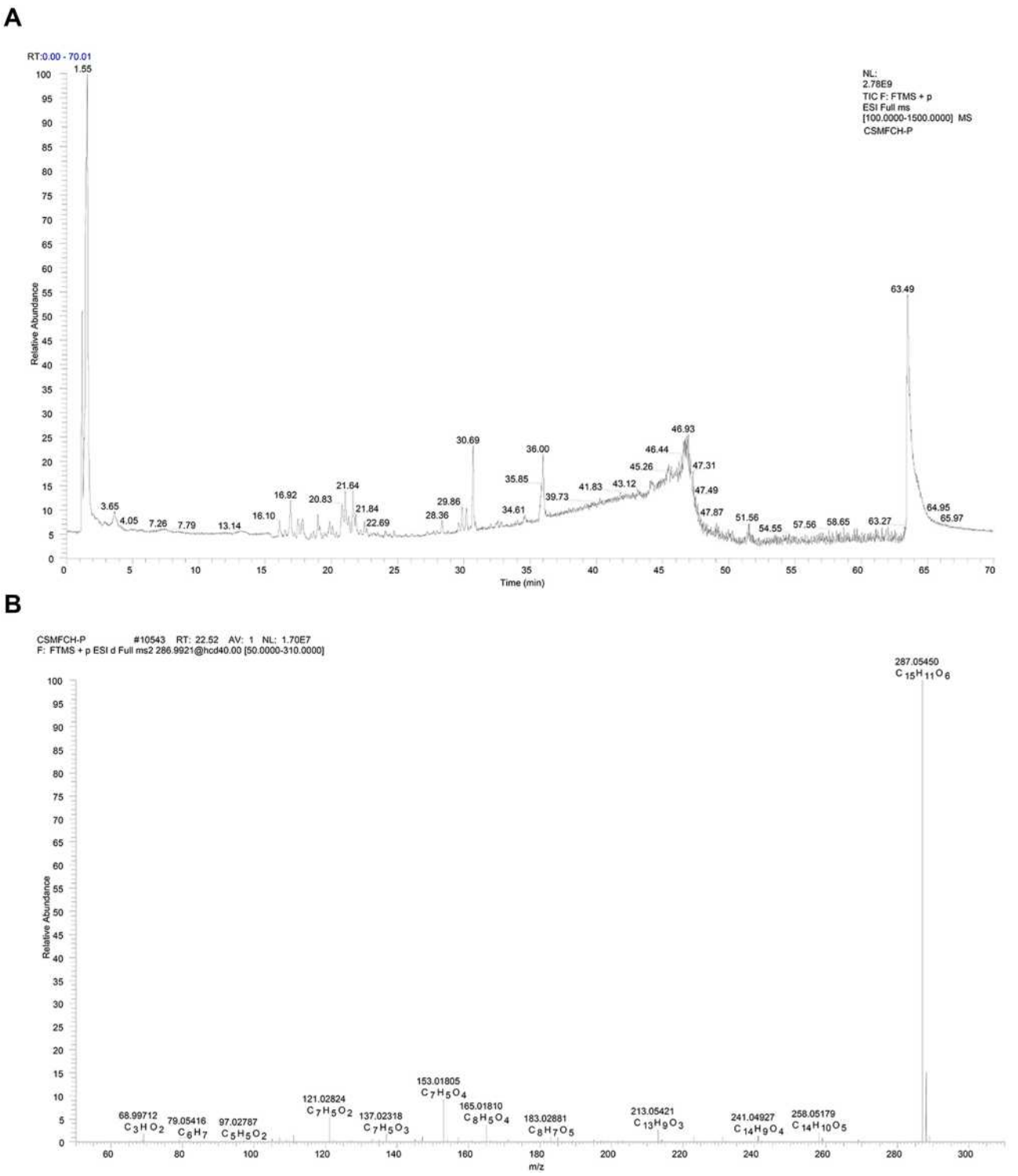

Figure 14 Mass spectrum of CSMFCH in the positive ion mode. (**A**) Total ion current chromatogram of CSMFCH. (**B**) ESI-MS/MS spectra of kaempferol.
Abbreviation: CSMFCH,*Cuscutae Semen-Mori Fructus* coupled-herbs.

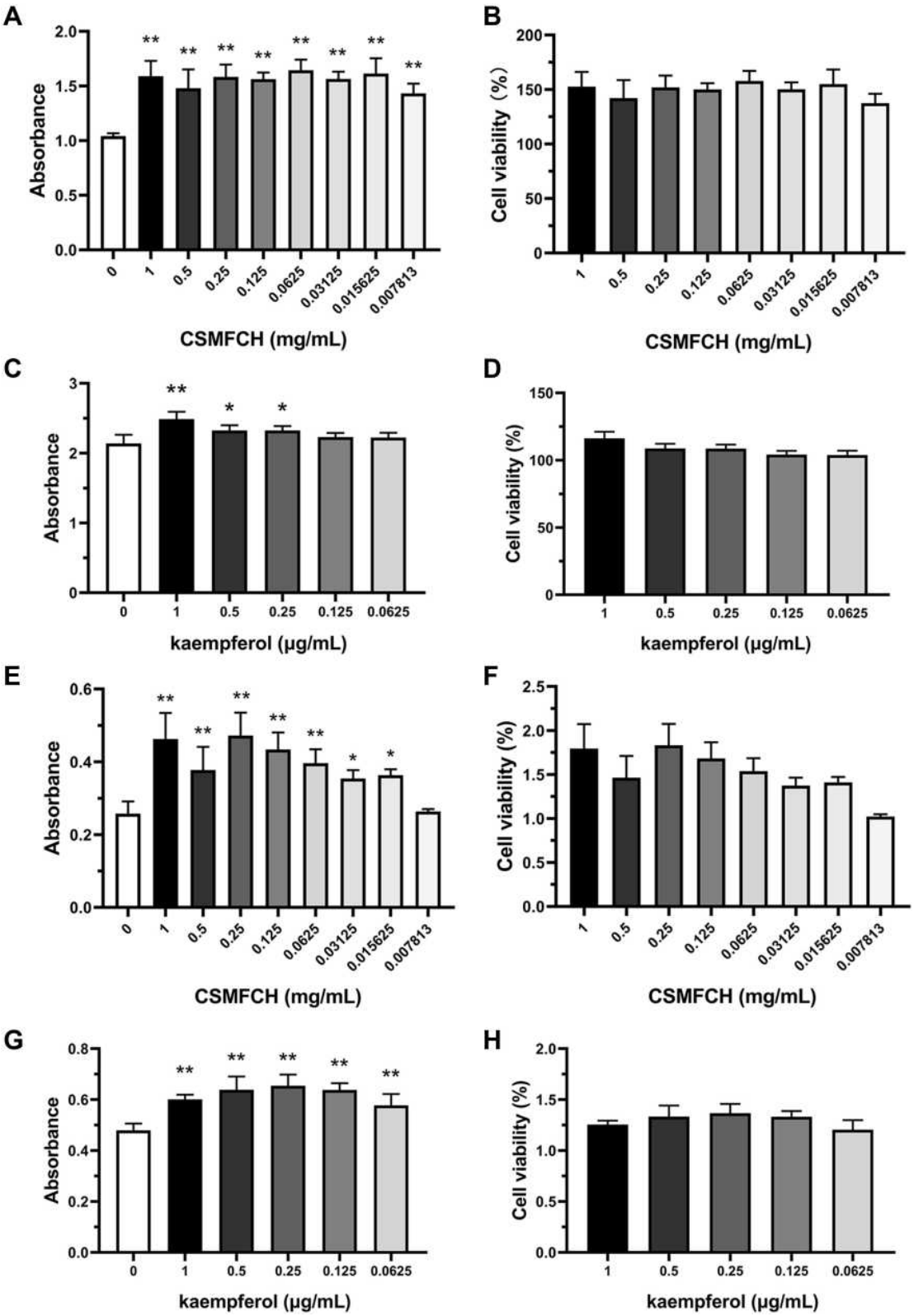

Figure 15 The absorbance and cell viability of TM3 and TM4 cells after CSMFCH and kaempferol treatment. (**A**) The absorbance of TM3 cells after CSMFCH treatment. (**B**) The cell viability of TM3 cells after CSMFCH treatment. (**C**) The absorbance of TM3 cells after kaempferol treatment. (**D**) The cell viability of TM3 cells after kaempferol treatment. (**E**) The absorbance of TM4 cells after CSMFCH treatment. (**F**) The cell viability of TM4 cells after CSMFCH treatment. (**G**) The absorbance of TM4 cells after kaempferol treatment. (**H**) The cell viability of TM4 cells after kaempferol treatment. Data: n = 6, mean ± SD, experiments performed in triplicate. *P < 0.05 and **P < 0.01 versus non-treatment control group.

Abbreviations: TM3, mouse Leydig; TM4, mouse Sertoli; CSMFCH,*Cuscutae Semen-Mori Fructus* coupled-herbs.

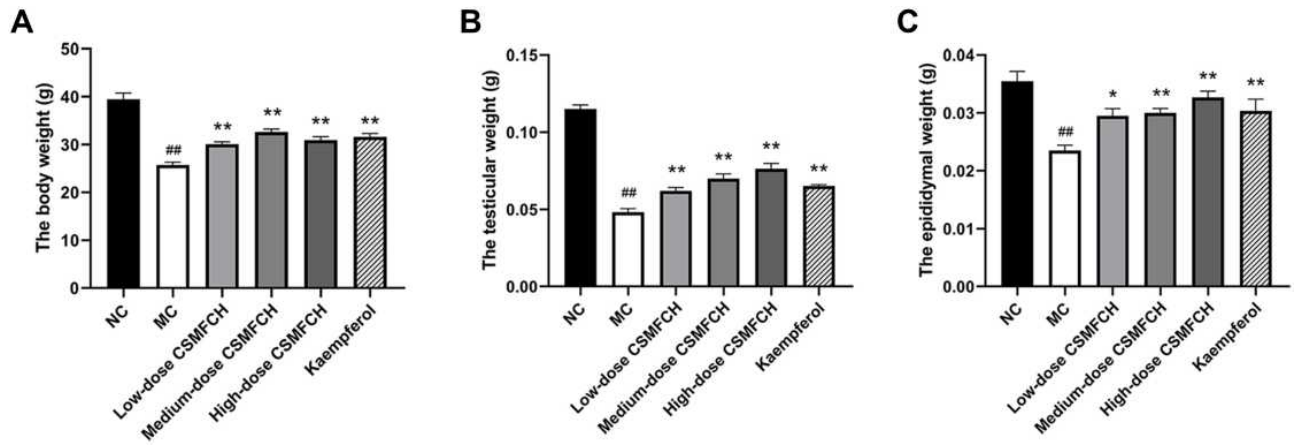

Figure 16 The body, testicular, and epididymal weight of each group. (**A**) The body weight. (**B**) The testicular weight. (**C**) The epididymal weight. Data: n = 6, mean ± SD, experiments performed in triplicate. $^{\#\#}P < 0.01$ versus the NC group, $^{*}P < 0.05$ and $^{**}P < 0.01$ versus the MC group.
Abbreviations: NC, normal control; MC, model control; CSMFCH,*Cuscutae Semen-Mori Fructus* coupled-herbs.

The Sperm Quality of OA Mice in the Treatment of CSMFCH and Kaempferol

Compared with the NC group, CP significantly decreased the density, viability, and motility of sperm, and increased the abnormal sperm motility in the MC group, indicating the successful establishment of the OA mouse model (all $P < 0.01$). The kaempferol group and low-, medium-, and high-dose CSMFCH groups significantly improved the density, viability, and motility of sperm, and decreased the abnormal sperm motility compared with the MC group (all $P < 0.01$). The results are presented in Figure 17. The sperm morphology is shown in Figure 18.

Histopathological Analysis of OA Mice in the Treatment of CSMFCH and Kaempferol

A histological analysis of testicular tissue from NC group revealed a normal process of spermatogenesis, with a regular arrangement of spermatogenic epithelial cells in the seminiferous tubules. In contrast, the MC group exhibited testicular damage including loss, disorganization, and sloughing of spermatogenic cells, degeneration of interstitial cells, and vacuolization in the cytoplasm of Sertoli cells, which were consistent with OA. CSMFCH and kaempferol administration partly restored the morphology of Leydig, Sertoli, and spermatogenic cells (Figure 19).

Discussion

Nowadays, with the improvement of living standards and modern medicine, more and more hard-to-cure diseases were conquered. However, the treatment of some diseases still faces challenges because of their unclear underlying molecular mechanism, including OA. Thus, new approaches or drugs for the therapy of OA ought to be developed, and the importance is emphasized by the current COVID-19 pandemic. TCM has attracted more and more attention to treating OA because of its "multi-component" and "multi-target" features. CSMFCH has been used in China for centuries for curing OA and serves as one of the most significant attributes of the anti-OA TCM formula. Nevertheless, the substantive basis and mechanism of CSMFCH against OA needs to be made clear. Hence, a comprehensive approach integrated network pharmacology, molecular docking, and experiment validation was performed to reveal the new candidate active component and mechanism of CSMFCH in the treatment of OA.

In this research, using online sources, a total of 153 predicted targets of 137 CSMFCH components and 495 OA-related targets were obtained. 64 CSMFCH-OA common targets were then screened to construct the CSMFCH-OA common-target network. After that, GO and KEGG pathway enrichment analyses were applied on the CSMFCH-OA component-target network, OA-related targets, CSMFCH-OA common-target network, PPI network, and clusters. We developed the core component-target-pathway network based on the findings above. According to the results, we forecast Kaempferol is the most significant component, and Estrogen signaling pathway is the core pathway of the network. Moreover, 6 core targets are AKT1, EGFR, MAPK3, ESR1, CYP19A1, and AR.

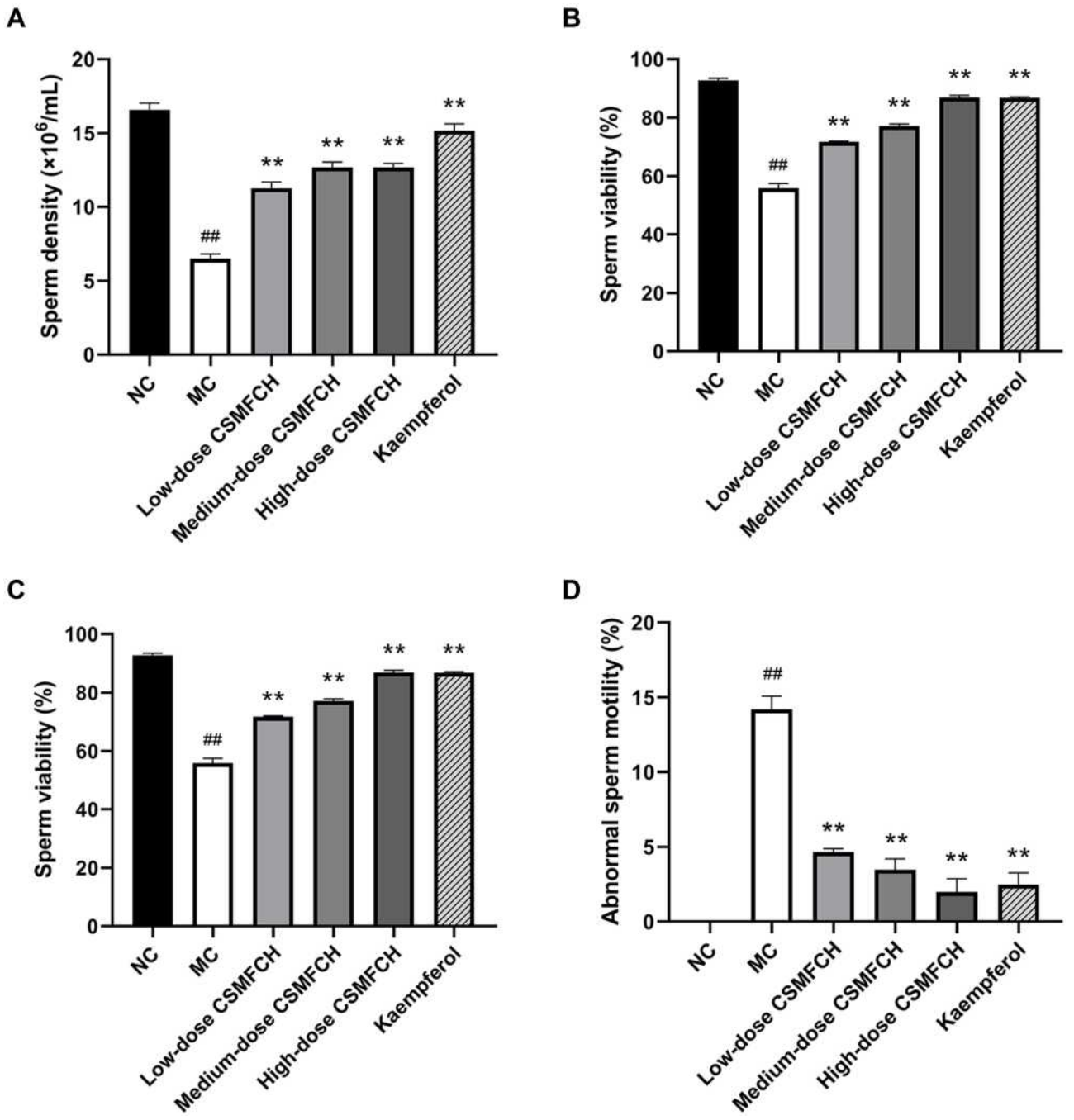

Figure 17 The sperm quality of each group. (**A**) The sperm density. (**B**) The sperm viability. (**C**) The sperm motility. (**D**) The abnormal sperm motility. Data: n = 6, mean ± SD, experiments performed in triplicate. $^{\#\#}P < 0.01$ versus the NC group, $^{**}P < 0.01$ versus the MC group.
Abbreviations: NC, normal control; MC, model control; CSMFCH,*Cuscutae Semen-Mori Fructus* coupled-herbs.

Molecular docking was utilized to verify the strong binding interactions between kaempferol and core targets. UHPLC-Q-Orbitrap-MS analysis was conducted to identify kaempferol in CSMFCH extract. CSMFCH and kaempferol both increased the viability in TM3 and TM4 cells. CSMFCH and kaempferol could improve male reproductive organ weights, the sperm quality, and decrease testis tissue damage in the CP-induced OA mouse model, which further verified the results of network pharmacology.

Specifically, kaempferol protects sperm from estrogen-induced oxidative DD.[79] An in vitro study showed that

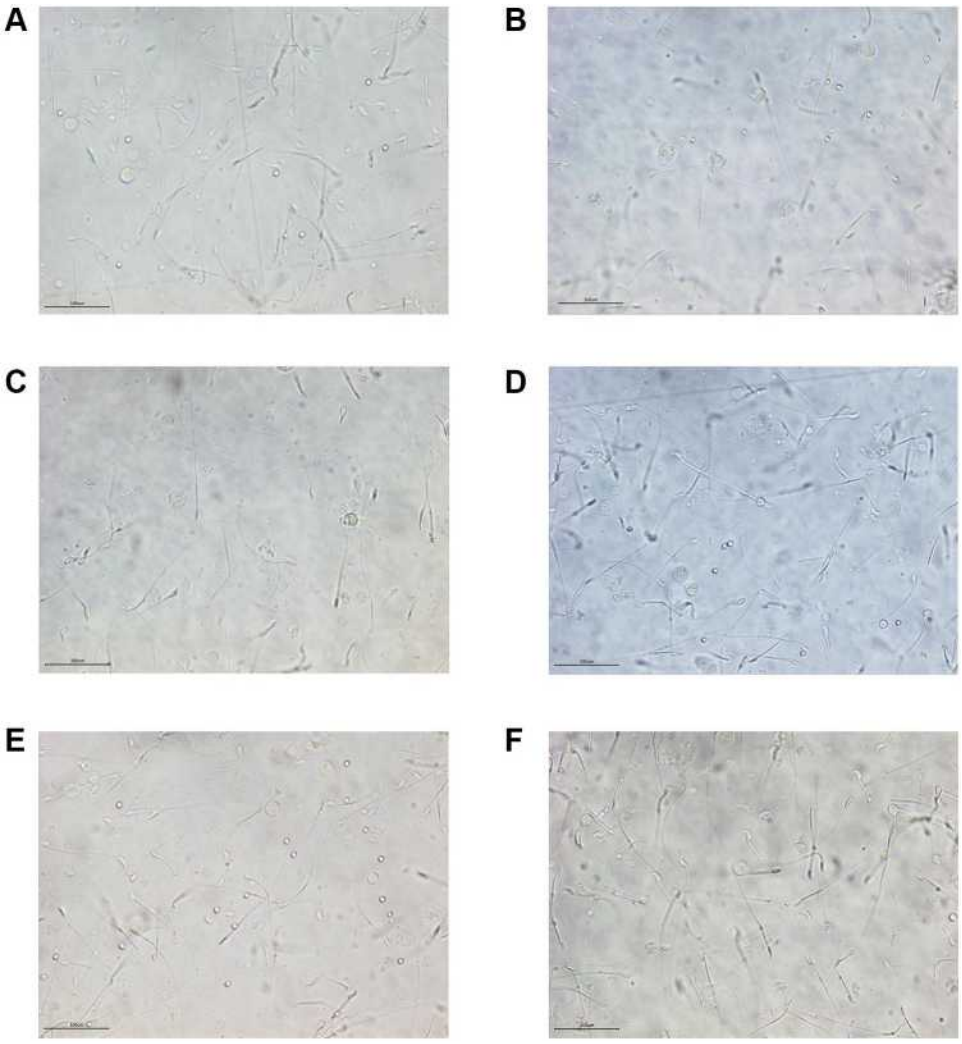

Figure 18 The sperm morphology (×400). (**A**) The normal control group. (**B**) The model control group. (**C**) The low-dose CSMFCH group. (**D**) The medium-dose CSMFCH group. (**E**) The high-dose CSMFCH group. (**F**) The kaempferol group. Data: n = 6, experiments performed in triplicate.
Abbreviation: CSMFCH,*Cuscutae Semen-Mori Fructus* coupled-herbs.

kaempferol restored motility of aluminum-exposed human sperm cells and decreased the levels of malondialdehyde (MDA) production, a lipid peroxidation marker.[80] In our study, we conducted UHPLC-Q-Orbitrap-MS approach to identify kaempferol in CSMFCH extract in negative and positive modes. It not only verified the result of network pharmacology, but also proved CSMFCH extract contains kaempferol.

Estrogen signaling pathway is the most notable signaling pathway. Estrogens are found to be involved in varicocele-related male infertility pathophysiology.[81] Estrogen stimulation can directly affect the apoptosis of germ cells, and it can also change the communication between germ cells to change their apoptosis,[82] which may have a profound impact on OA. The core targets of CSMFCH against OA are AKT1, EGFR, MAPK3, ESR1, CYP19A1, and AR. AKT1 is considered as the moderator of cellular growth, survival, metabolism and proliferation.[83] In vivo, AKT1 also inhibits radiation-induced germ cell apoptosis and boosts the impact of thyroid hormone on the growth of postnatal testis.[84,85] In the capacitation process, the EGFR is partially activated by protein kinase A (PKA), resulting in phospholipase D (PLD) activation and actin polymerization.[86] In human, MAPK3 plays a crucial role in cell cycle progression and apoptosis.[87] The MAPKs has been linked to disturbances in spermatogenesis and dysfunction of germ cells and Sertoli cells, resulting in reduced semen quality and male reproductive dysfunction.[88] ESR1 could regulate expression of genes during the process of spermiogenesis,

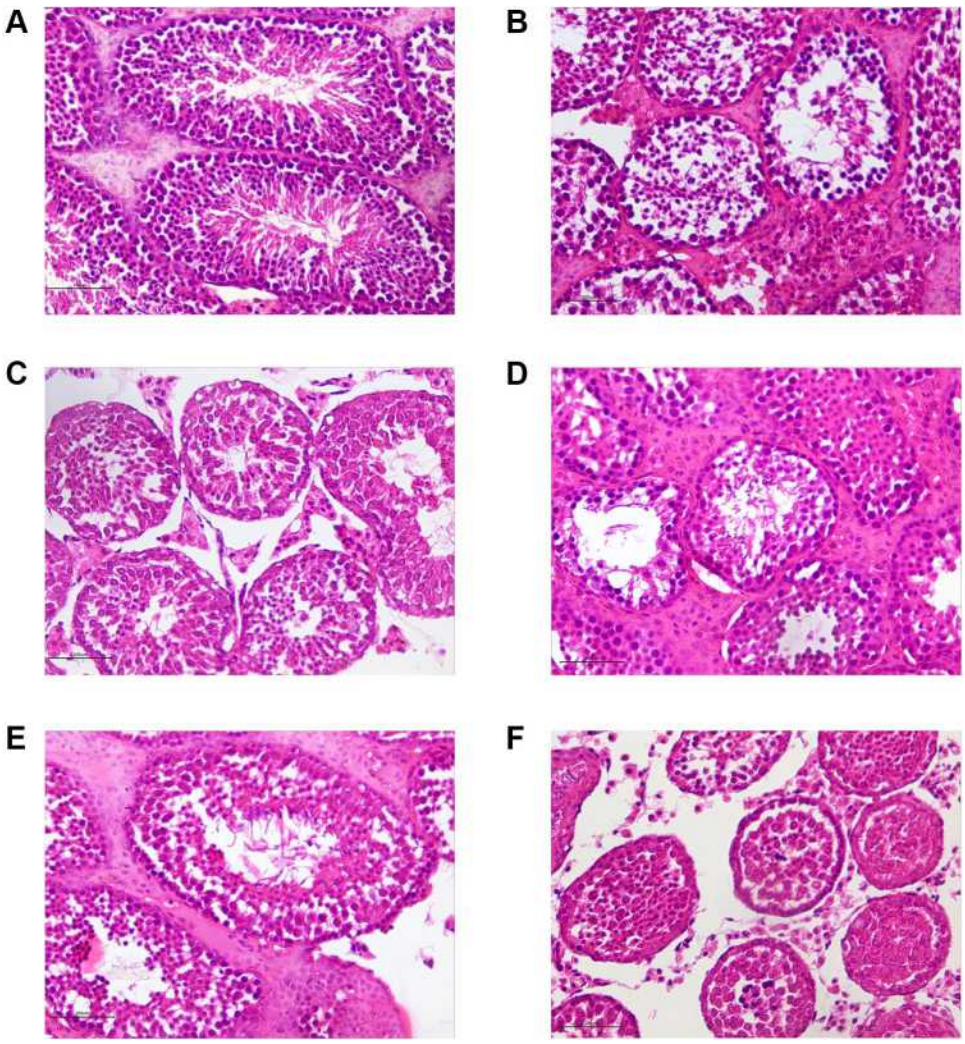

Figure 19 HE staining of testicular tissues (×400). (**A**) The normal control group. (**B**) The model control group. (**C**) The low-dose CSMFCH group. (**D**) The medium-dose CSMFCH group. (**E**) The high-dose CSMFCH group. (**F**) The kaempferol group. Data: n = 6, experiments performed in triplicate.
Abbreviation: CSMFCH,*Cuscutae Semen-Mori Fructus* coupled-herbs.

and has been implicated in male infertility.[89–91] In addition, ESR1 has been shown to be associated with cancer of testicular germ cells, which typically occurs in young males.[92] Cytochrome P450 aromatase, a result of the CYP19A1 gene, regulates the equilibrium between androgen and estrogen necessary for normal male reproductive development.[93] For the development and production of the male phenotype and spermatogenesis, AR is crucially important.[94,95] Prior studies have shown that AR could act through testicular Sertoli and peritubular myoid cells, explicitly preserving the amount of spermatogonia, the integrity of the blood-testis barrier, meiosis completion, sperm adhesion.[96,97]

TM3 cells are non-cancerous cells with receptor sites of LH, AR, ER and growth factor, resulting in cholesterol metabolism.[98] Synthesizing and secreting androgenic steroids is the primary function of TM3 cells. Testosterone, which is necessary for the process of spermatogenesis, is the main male steroid hormone.[99,100] Sertoli cells in the basal segment of seminiferous tubules play an important role in testicular and spermatogenesis. In addition, they secrete functional proteins and hormones to suppress and distinguish spermatogonia, including inhibin B and anti-Mullerian hormone.[101,102] The number of Sertoli cells defines the population size of germ cells, which is essential for the maintenance of spermatogenesis and consequently, male fertility.[103] Therefore, TM3 and TM4 cells play an essential role in pathogenesis of OA and male infertility. In our study, two different testicular cells, TM3 and TM4 cells, were used to analyze the effects of CSMFCH and

kaempferol on OA. The results showed that CSMFCH and kaempferol could increase the cell viability of TM3 and TM4 cells.

CP is a new chemotherapy drug that reduces fertility in treated patients.[104–106] CP may have a detrimental impact on the tissue and epididymis, according to the previous research.[107] It may also impair the production of sperm in the testes and the maturation of sperm in the epididymis.[108] Patients treated with CP for four months or longer have undergone different OA conditions.[109] CP had the most harmful effects on the tests.[110] Sperm consistency and fertility are two of the most serious side effects of CP as an alkylating agent and cytotoxic drug.[111] CP treatment can affect the sperm features of male animals.[112] CSMFCH and kaempferol could improve the male reproductive organ weights, sperm quality, and decrease testis tissue damage in the OA mouse model induced by CP, which further verified the results of network pharmacology.

Conclusion

In summary, the new candidate active component and mechanism of CSMFCH against OA were revealed by an integrated analysis, comprising network pharmacology approach, molecular docking method, UHPLC-Q-Orbitrap-MS identification, TM3 and TM4 experimental validation. According to the results, we assumed that kaempferol is the new candidate active component of CSMFCH in the treatment of OA. Hormone regulation, OS reduction, and male productive promotion are related to the mechanism and targets of CSMFCH on OA. Among them, the most notable signaling pathway is estrogen signaling pathway. AKT1, EGFR, MAPK3, ESR1, CYP19A1, and AR are the core potential targets during the process of CSMFCH on OA. Furthermore, molecular docking verified the strong binding interaction between kaempferol and core potential targets. Kaempferol of CSMFCH was identified by UHPLC-Q-Orbitrap-MS technology. Furthermore, CSMFCH and kaempferol could enhance the mouse Leydig (TM3) and mouse Sertoli (TM4) cell viability, improve the male reproductive organ weights, sperm quality, and decrease testis tissue damage in the OA mouse model induced by CP, which verified the results of network pharmacology.

Acknowledgments

This research was funded by the Longitudinal Development Project of Beijing University of Chinese Medicine, grant number 2018-zxfzjj-002 and 81373780, the project of Beijing University of Chinese Medicine and Beijing Tong Ren Tang Company Limited Scientific Research Institute, grant number 2020071720310, the Beijing Natural Science Foundation, grant number 7202115, and the Innovation Team Project of Beijing University of Chinese Medicine, grant number 2019-JYB-TD010.

Disclosure

The authors report no conflicts of interest in this work.

References

1. Zegers-Hochschild F, Adamson GD, de Mouzon J, et al. The International Committee for Monitoring Assisted Reproductive Technology (ICMART) and the World Health Organization (WHO) Revised Glossary on ART Terminology, 2009. *Hum Reprod*. 2009;24(11):2683–2687. doi:10.1093/humrep/dep343
2. Dohle GR, Colpi GM, Hargreave TB, et al. EAU guidelines on male infertility. *Eur Urol*. 2005;48(5):703–711. doi:10.1016/j.eururo.2005.06.002
3. Amory J, Ostrowski K, Gannon J, et al. Isotretinoin administration improves sperm production in men with infertility from oligoasthenozoospermia: a pilot study. *Andrology*. 2017;5(6):1115–1123. doi:10.1111/andr.12420
4. Cooper TG, Noonan E, von Eckardstein S, et al. World Health Organization reference values for human semen characteristics. *Hum Reprod Update*. 2010;16(3):231–245. doi:10.1093/humupd/dmp048
5. Machen GL, Sandlow JI. Causes of male infertility. *Male Infertility Springer*. 2020;3–14.
6. Tournaye H, Krausz C, Oates RD. Concepts in diagnosis and therapy for male reproductive impairment. *Lancet Diabetes Endocrinol*. 2017;5(7):554–564. doi:10.1016/S2213-8587(16)30043-2
7. Singh B, Reschke L, Segars J, Baker VL. Frozen-thawed embryo transfer: the potential importance of the corpus luteum in preventing obstetrical complications. *Fertil Steril*. 2020;113(2):252–257. doi:10.1016/j.fertnstert.2019.12.007
8. Illiano E, Trama F, Costantini E. Could COVID-19 have an impact on male fertility? *Andrologia*. 2020;e13654. doi:10.1111/and.13654
9. Wang S, Zhou X, Zhang T, Wang Z. The need for urogenital tract monitoring in COVID-19. *Nat Rev Urol*. 2020;1–2. doi:10.1038/s41585-020-0319-7
10. Segars J, Katler Q, McQueen DB, et al. Prior and novel coronaviruses, COVID-19, and human reproduction: what is known? *Fertil Steril*. 2020. doi:10.1016/j.fertnstert.2020.04.025
11. Xu J, Qi L, Chi X, et al. Orchitis: a complication of severe acute respiratory syndrome (SARS). *Biol Reprod*. 2006;74(2):410–416. doi:10.1095/biolreprod.105.044776
12. Youssef K, Abdelhak K. Male genital damage in COVID-19 patients: are available data relevant? *Asian J Urol*. 2020. doi:10.1016/j.ajur.2020.06.005
13. Aitken RJ. COVID-19 and human spermatozoa–potential risks for infertility and sexual transmission. *Andrology*. 2020;1–5. doi:10.1111/andr.12859
14. Starc A, Trampuš M, Pavan Jukić D, Grgas-Bile C, Jukić T, Polona Mivšek A. Infertility and sexual dysfunctions: a systematic literature review. *Acta Clinica Croatica*. 2019;58(3):508–515. doi:10.20471/acc.2019.58.03.15

15. Foresta C, Bettella A, Merico M, Garolla A, Ferlin A, Rossato M. Use of recombinant human follicle-stimulating hormone in the treatment of male factor infertility. *Fertil Steril*. 2002;77(2):238–244. doi:10.1016/s0015-0282(01)02966-1
16. Henkel R, Sandhu IS, Agarwal A. The excessive use of antioxidant therapy: a possible cause of male infertility? *Andrologia*. 2019;51(1):e13162. doi:10.1111/and.13162
17. Helo S, Ellen J, Mechlin C, et al. A randomized prospective double-blind comparison trial of clomiphene citrate and anastrozole in raising testosterone in hypogonadal infertile men. *J Sex Med*. 2015;12(8):1761–1769. doi:10.1111/jsm.12944
18. Jung JH, Seo JT. Empirical medical therapy in idiopathic male infertility: promise or panacea? *Clin Exp Reprod Med*. 2014;41(3):108. doi:10.5653/cerm.2014.41.3.108
19. Wang M, Wang Q, Du Y, Jiang H, Zhang X. Vitamins combined with traditional Chinese medicine for male infertility: a systematic review and meta-analysis. *Andrology*. 2020;8(5):1038–1050. doi:10.1111/andr.12787
20. Nagata M, Suzuki T. L-carnitine partially improves metabolic syndrome symptoms but does not re-verse perturbed sperm function or infertility in high fat diet-induced obese mice. *MJ Nutr*. 2017;2(1):013.
21. Qin J, Sheng X, Wang H, Liang D, Tan H, Xia J. Assisted reproductive technology and risk of congenital malformations: a meta-analysis based on cohort studies. *Arch Gynecol Obstet*. 2015;292(4):777–798. doi:10.1007/s00404-015-3707-0
22. Jiang D, Coscione A, Li L, Zeng B-Y. Effect of Chinese herbal medicine on male infertility. *Int Rev Neurobiol Elsevier*. 2017;297–311.
23. Jin X, Man C, Gong D, Fan Y. Adjuvant treatment with Qilin pill for men with oligoasthenospermia: a meta-analysis of randomized controlled trials. *Phytother Res*. 2017;31(9):1291–1297. doi:10.1002/ptr.5854
24. Zhou S, Weng Z, Liang A, Zhang S. Experimental research on therapeutic efficacy of traditional chinese medicine Shengjing Capsule extracts in treating spermatogenesis impairment induced by oxidative stress. *Med Sci Monitor*. 2016;22:50. doi:10.12659/MSM.895336
25. Lin M-K, Lee M-S, Chang W-T, Yang M-C, Chu C-L. Study the immunomodulatory activity of semen cuscutae and identify the active components. *J Biosci Bioeng*. 2009;108:S19. doi:10.1016/j.jbiosc.2009.08.492
26. Yang S, Xu X, Xu H, et al. Purification, characterization and biological effect of reversing the kidney-yang deficiency of polysaccharides from semen cuscutae. *Carbohydr Polym*. 2017;175:249–256. doi:10.1016/j.carbpol.2017.07.077
27. Jian-Hui L, Bo J, Yong-Ming B, Li-Jia A. Effect of Cuscuta chinensis glycoside on the neuronal differentiation of rat pheochromocytoma PC12 cells. *Int J Develop Neurosci*. 2003;21(5):277–281. doi:10.1016/S0736-5748(03)00040-6
28. Nisa M, Akbar S, Tariq M, Hussain Z. Effect of Cuscuta chinensis water extract on 7, 12-dimethylbenz [a] anthracene-induced skin papillomas and carcinomas in mice. *J Ethnopharmacol*. 1986;18(1):21–31. doi:10.1016/0378-8741(86)90040-1
29. Lee JS, Synytsya A, Kim HB, et al. Purification, characterization and immunomodulating activity of a pectic polysaccharide isolated from Korean mulberry fruit Oddi (Morus alba L. *Int Immunopharmacol*. 2013;17(3):858–866. doi:10.1016/j.intimp.2013.09.019
30. Chen C, You L-J, Huang Q, et al. Modulation of gut microbiota by mulberry fruit polysaccharide treatment of obese diabetic db/db mice. *Food Funct*. 2018;9(7):3732–3742. doi:10.1039/C7FO01346A
31. Chen Y, Yao F, Ming K, Wang D, Hu Y, Liu J. Polysaccharides from traditional Chinese medicines: extraction, purification, modification, and biological activity. *Molecules*. 2016;21(12):1705. doi:10.3390/molecules21121705
32. Zhao S, Iyengar R. Systems pharmacology: network analysis to identify multiscale mechanisms of drug action. *Annu Rev Pharmacol Toxicol*. 2012;52:505–521. doi:10.1146/annurev-pharmtox-010611-134520
33. van Hasselt JGC, Iyengar R. Systems pharmacology: defining the interactions of drug combinations. *Annu Rev Pharmacol Toxicol*. 2019;59:21–40. doi:10.1146/annurev-pharmtox-010818-021511
34. Hopkins AL. Network pharmacology: the next paradigm in drug discovery. *Nat Chem Biol*. 2008;4(11):682. doi:10.1038/nchembio.118
35. Shao L, Zhang B. Traditional Chinese medicine network pharmacology: theory, methodology and application. *Chin J Nat Med*. 2013;11(2):110–120. doi:10.1016/S1875-5364(13)60037-0
36. Li J, Fu A, Zhang L. An overview of scoring functions used for protein–ligand interactions in molecular docking. *Interdiscip Sci*. 2019;1–9. doi:10.1007/s12539-019-00327-w
37. Ru J, Li P, Wang J, et al. TCMSP: a database of systems pharmacology for drug discovery from herbal medicines. *J Cheminform*. 2014;6:13. doi:10.1186/1758-2946-6-13
38. Huang L, Xie D, Yu Y, et al. TCMID 2.0: a comprehensive resource for TCM. *Nucleic Acids Res*. 2018;46(D1):D1117–D1120. doi:10.1093/nar/gkx1028
39. Feng W, Ao H, Yue S, Peng C. Systems pharmacology reveals the unique mechanism features of Shenzhu Capsule for treatment of ulcerative colitis in comparison with synthetic drugs. *Sci Rep*. 2018;8(1):16160. doi:10.1038/s41598-018-34509-1
40. Zhang X, Shen Y, Wang X, Yuan G, Zhang C, Yang Y. A novel homozygous CFAP65 mutation in humans causes male infertility with multiple morphological abnormalities of the sperm flagella. *Clin Genet*. 2019;96(6):541–548. doi:10.1111/cge.13644
41. Li H, Zhao L, Zhang B, et al. A network pharmacology approach to determine active compounds and action mechanisms of ge-gen-qin-lian decoction for treatment of type 2 diabetes. *Evidence-Based Compl Alternative Med*. 2014;2014:1–12.
42. Zuo H, Zhang Q, Su S, Chen Q, Yang F, Hu Y. A network pharmacology-based approach to analyse potential targets of traditional herbal formulas: an example of Yu Ping Feng decoction. *Sci Rep*. 2018;8(1):1–15. doi:10.1038/s41598-018-29764-1
43. Xu X, Zhang W, Huang C, et al. A novel chemometric method for the prediction of human oral bioavailability. *Int J Mol Sci*. 2012;13(6):6964–6982. doi:10.3390/ijms13066964
44. Walters WP, Murcko MA. Prediction of 'drug-likeness'. *Adv Drug Deliv Rev*. 2002;54(3):255–271. doi:10.1016/s0169-409x(02)00003-0
45. Bardou P, Mariette J, Escudié F, Djemiel C, Klopp C. jvenn: an interactive Venn diagram viewer. *BMC Bioinform*. 2014;15(1):1–7. doi:10.1186/1471-2105-15-293
46. Kim S, Chen J, Cheng T, et al. PubChem 2019 update: improved access to chemical data. *Nucleic Acids Res*. 2019;47(D1):D1102–D1109. doi:10.1093/nar/gky1033
47. Tetko IV, Poda GI. Application of ALOGPS 2.1 to predict log D distribution coefficient for Pfizer proprietary compounds. *J Med Chem*. 2004;47(23):5601–5604. doi:10.1021/jm049509l
48. Gfeller D, Grosdidier A, Wirth M, Daina A, Michielin O, Zoete V. SwissTargetPrediction: a web server for target prediction of bioactive small molecules. *Nucleic Acids Res*. 2014;42(Web Server issue):W32–8. doi:10.1093/nar/gku293
49. UniProt C. UniProt: a hub for protein information. *Nucleic Acids Res*. 2015;43(Database issue):D204–12. doi:10.1093/nar/gku989
50. Shannon P, Markiel A, Ozier O, et al. Cytoscape: a software environment for integrated models of biomolecular interaction networks. *Genome Res*. 2003;13(11):2498–2504. doi:10.1101/gr.1239303
51. Assenov Y, Ramirez F, Schelhorn SE, Lengauer T, Albrecht M. Computing topological parameters of biological networks. *Bioinformatics*. 2008;24(2):282–284. doi:10.1093/bioinformatics/btm554

52. Pinero J, Bravo A, Queralt-Rosinach N, et al. DisGeNET: a comprehensive platform integrating information on human disease-associated genes and variants. *Nucleic Acids Res*. 2017;45(D1):D833–D839. doi:10.1093/nar/gkw943
53. Davis AP, Grondin CJ, Johnson RJ, et al. The Comparative Toxicogenomics Database: update 2019. *Nucleic Acids Res*. 2019;47(D1):D948–D954. doi:10.1093/nar/gky868
54. Amberger JS, Hamosh A. Searching Online Mendelian Inheritance in Man (OMIM): a knowledgebase of human genes and genetic phenotypes. *Curr Protoc Bioinformatics*. 2017;58:1 2 1–1 2 12. doi:10.1002/cpbi.27
55. Stelzer G, Rosen N, Plaschkes I, et al. The genecards suite: from gene data mining to disease genome sequence analyses. *Curr Protoc Bioinformatics*. 2016;54:1 30 1–1 30 33. doi:10.1002/cpbi.5
56. Brown GR, Hem V, Katz KS, et al. Gene: a gene-centered information resource at NCBI. *Nucleic Acids Res*. 2015;43 (Database issue):D36–42. doi:10.1093/nar/gku1055
57. Yang Z, Zhang X, Chen Z, Hu C. Effect of Wuzi Yanzong on Reproductive Hormones and TGF-beta1/Smads signal pathway in rats with oligoasthenozoospermia. *Evid Based Complement Alternat Med*. 2019;2019:7628125. doi:10.1155/2019/7628125
58. Szklarczyk D, Franceschini A, Wyder S, et al. STRING v10: protein-protein interaction networks, integrated over the tree of life. *Nucleic Acids Res*. 2015;43(Database issue):D447–52. doi:10.1093/nar/gku1003
59. Bader GD, Hogue CW. An automated method for finding molecular complexes in large protein interaction networks. *BMC Bioinform*. 2003;4:2. doi:10.1186/1471-2105-4-2
60. Ahmed HA, Bhattacharyya DK, Kalita JK. Core and peripheral connectivity based cluster analysis over PPI network. *Comput Biol Chem*. 2015;59(Pt):B:32–41. doi:10.1016/j.compbiolchem.2015.08.008
61. The Gene Ontology C. Expansion of the Gene Ontology knowledgebase and resources. *Nucleic Acids Res*. 2017;45(D1):D331–D338. doi:10.1093/nar/gkw1108.
62. Du J, Yuan Z, Ma Z, Song J, Xie X. KEGG-PATH: kyoto encyclopedia of genes and genomes-based pathway analysis using a path analysis model. *Mol Biosyst*. 2014;10 (9):2441–2447. doi:10.1039/c4mb00287c
63. Zhou Y, Zhou B, Pache L, et al. Metascape provides a biologist-oriented resource for the analysis of systems-level datasets. *Nat Commun*. 2019;10(1):1–10. doi:10.1073/pnas.1822164116
64. Wilson CL, Miller CJ. Simpleaffy: a bioconductor package for affymetrix quality control and data analysis. *Bioinformatics*. 2005;21(18):3683–3685. doi:10.1093/bioinformatics/bti605
65. Bindea G, Mlecnik B, Hackl H, et al. ClueGO: a Cytoscape plug-in to decipher functionally grouped gene ontology and pathway annotation networks. *Bioinformatics*. 2009;25(8):1091–1093. doi:10.1093/bioinformatics/btp101
66. Berman HM, Westbrook J, Feng Z, et al. The protein data bank. *Nucleic Acids Res*. 2000;28(1):235–242. doi:10.1093/nar/28.1.235
67. Yuan S, Chan HCS, Filipek S, Vogel H. PyMOL and inkscape bridge the data and the data visualization. *Structure*. 2016;24 (12):2041–2042. doi:10.1016/j.str.2016.11.012
68. Trott O, Olson AJ. AutoDock Vina: improving the speed and accuracy of docking with a new scoring function, efficient optimization, and multithreading. *J Comput Chem*. 2010;31 (2):455–461. doi:10.1002/jcc.21334
69. Lan R, Xiang J, Wang G-H, et al. Xiao-Xu-Ming decoction protects against blood-brain barrier disruption and neurological injury induced by cerebral ischemia and reperfusion in rats. *Evidence-Based Compl Alternative Med*. 2013;2013.
70. Zhang Q, Zhao H, Wang L, Zhang Q, Wang H. Effects of wind-dispelling drugs and deficiency-nourishing drugs of Houshiheisan compound prescription on astrocyte activation and inflammatory factor expression in the corpus striatum of cerebral ischemia rats. *Neural Regeneration Res*. 2012;7(24):1851.
71. Wang Y, Xiao J, Suzek TO, Zhang J, Wang J, Bryant SH. PubChem: a public information system for analyzing bioactivities of small molecules. *Nucleic Acids Res*. 2009;37(suppl_2):W623–W633. doi:10.1093/nar/gkp456
72. Akram H, Pakdel FG, Ahmadi A, Zare S. Beneficial effects of american ginseng on epididymal sperm analyses in cyclophosphamide treated rats. *Cell Journal (Yakhteh)*. 2012;14(2):116.
73. Bakhtiary Z, Shahrooz R, Ahmadi A, Zarei L. Evaluation of antioxidant effects of crocin on sperm quality in cyclophosphamide treated adult mice. Faculty of Veterinary Medicine, Urmia University, Urmia, Iran. *Veterinary Res Forum Int Quart J*. 2014;(3):213.
74. Zhao H, Jin B, Zhang X, et al. Yangjing capsule ameliorates spermatogenesis in male mice exposed to cyclophosphamide. *Evidence-Based Compl Alternative Med*. 2015;2015:1–8. doi:10.1155/2015/980583
75. Yan G, Tian F, Liu P, et al. Sheng Jing Decoction, as a Traditional Chinese Medicine Prescription, Can Promote Spermatogenesis and Increase Sperm Motility. *Research Square*. 2021:1–16. doi:10.21203/rs.3.rs-167175/v1.
76. Mehraban Z, Ghaffari Novin M, Golmohammadi MG, Sagha M, Pouriran K, Nazarian H. Protective effect of gallic acid on apoptosis of sperm and in vitro fertilization in adult male mice treated with cyclophosphamide. *J Cell Biochem*. 2019;120 (10):17250–17257. doi:10.1002/jcb.28987
77. Chang Z, Bai X, Tang Y, et al. Pharmacological mechanisms of Yishen Xingyang capsule in the treatment of oligoasthenospermia in rats. *J Traditional Chinese Med Sci*. 2021;8(1):52–58. doi:10.1016/j.jtcms.2021.01.004
78. Yang B, Yang Y-S, Yang N, Li G, Zhu H-L. Design, biological evaluation and 3D QSAR studies of novel dioxin-containing pyrazoline derivatives with thiourea skeleton as selective HER-2 inhibitors. *Sci Rep*. 2016;6(1):1–12. doi:10.1038/srep27571
79. Anderson D, Schmid TE, Baumgartner A, Cemeli-Carratala E, Brinkworth MH, Wood JM. Oestrogenic compounds and oxidative stress (in human sperm and lymphocytes in the Comet assay). *Mutation Res Rev Mutation Res*. 2003;544(2–3):173–178. doi:10.1016/j.mrrev.2003.06.016
80. Jamalan M, Ghaffari MA, Hoseinzadeh P, Hashemitabar M, Zeinali M. Human sperm quality and metal toxicants: protective effects of some flavonoids on male reproductive function. *Int j Fertility Sterility*. 2016;10(2):215.
81. Guido C, Perrotta I, Panza S, et al. Human sperm physiology: estrogen receptor alpha (ERα) and estrogen receptor beta (ERβ) influence sperm metabolism and may be involved in the pathophysiology of varicocele-associated male infertility. *J Cell Physiol*. 2011;226(12):3403–3412. doi:10.1002/jcp.22703
82. Alves MRC. Estrogens Regulate the Survival and Death Communication Between Sertoli and Germ Cells: A Clue for Male Infertility? Universidade da Beira Interior; 2013.
83. Poplinski A, Tüttelmann F, Kanber D, Horsthemke B, Gromoll J. Idiopathic male infertility is strongly associated with aberrant methylation of MEST and IGF2/H19 ICR1. *Int J Androl*. 2010;33(4):642–649. doi:10.1111/j.1365-2605.2009.01000.x
84. Rasoulpour T, DiPalma K, Kolvek B, Hixon M. Akt1 suppresses radiation-induced germ cell apoptosis in vivo. *Endocrinology*. 2006;147(9):4213–4221. doi:10.1210/en.2006-0174

85. Santos-Ahmed J, Brown C, Smith SD, et al. Akt1 protects against germ cell apoptosis in the postnatal mouse testis following lactational exposure to 6-N-propylthiouracil. *Reprod Toxicol*. 2011;31(1):17–25. doi:10.1016/j.reprotox.2010.09.012
86. Breitbart H, Etkovitz N. Role and regulation of EGFR in actin remodeling in sperm capacitation and the acrosome reaction. *Asian J Androl*. 2011;13(1):106–110. doi:10.1038/aja.2010.78
87. Cocchia N, Pasolini M, Mancini R, et al. Effect of sod (superoxide dismutase) protein supplementation in semen extenders on motility, viability, acrosome status and ERK (extracellular signal-regulated kinase) protein phosphorylation of chilled stallion spermatozoa. *Theriogenology*. 2011;75(7):1201–1210. doi:10.1016/j.theriogenology.2010.11.031
88. Li MW, Mruk DD, Cheng CY. Mitogen-activated protein kinases in male reproductive function. *Trends Mol Med*. 2009;15(4):159–168. doi:10.1016/j.molmed.2009.02.002
89. Dumasia K, Kumar A, Deshpande S, Sonawane S, Balasinor N. Differential roles of estrogen receptors, ESR1 and ESR2, in adult rat spermatogenesis. *Mol Cell Endocrinol*. 2016;428:89–100. doi:10.1016/j.mce.2016.03.024
90. Joseph A, Hess RA, Schaeffer DJ, et al. Absence of estrogen receptor alpha leads to physiological alterations in the mouse epididymis and consequent defects in sperm function. *Biol Reprod*. 2010;82(5):948–957. doi:10.1095/biolreprod.109.079889
91. Joseph A, Shur BD, Ko C, Chambon P, Hess RA. Epididymal hypo-osmolality induces abnormal sperm morphology and function in the estrogen receptor alpha knockout mouse. *Biol Reprod*. 2010;82(5):958–967. doi:10.1095/biolreprod.109.080366
92. Brokken LJS, Lundberg-Giwercman Y, De-meyts ER, et al. Association of polymorphisms in genes encoding hormone receptors ESR1, ESR2 and LHCGR with the risk and clinical features of testicular germ cell cancer. *Mol Cell Endocrinol*. 2012;351(2):279–285. doi:10.1016/j.mce.2011.12.018
93. Li X, Li H, Jia L, Li X, Rahman N. Oestrogen action and male fertility: experimental and clinical findings. *Cell Mol Life Sci*. 2015;72(20):3915–3930. doi:10.1007/s00018-015-1981-4
94. Ferlin A, Vinanzi C, Garolla A, et al. Male infertility and androgen receptor gene mutations: clinical features and identification of seven novel mutations. *Clin Endocrinol (Oxf)*. 2006;65(5):606–610. doi:10.1111/j.1365-2265.2006.02635.x
95. Dohle G, Smit M, Weber R. Androgens and male fertility. *World J Urol*. 2003;21(5):341–345. doi:10.1007/s00345-003-0365-9
96. O'Hara L, Smith LB. Androgen receptor roles in spermatogenesis and infertility. *Best Pract Res Clin Endocrinol Metab*. 2015;29(4):595–605. doi:10.1016/j.beem.2015.04.006
97. Yong E, Loy C, Sim K. Androgen receptor gene and male infertility. *Hum Reprod Update*. 2003;9(1):1–7. doi:10.1093/humupd/dmg003
98. Matfier JP. Establishment and characterization of two distinct mouse testicular epithelial cell line. *Biol Reprod*. 1980;23(1):243–252. doi:10.1095/biolreprod23.1.243
99. Hess RA, De Franca LR. Spermatogenesis and cycle of the seminiferous epithelium. *Mol Mechanisms Spermatogenesis*. 2009;1–15.
100. Mathur PP, D'cruz SC. The effect of environmental contaminants on testicular function. *Asian J Androl*. 2011;13(4):585. doi:10.1038/aja.2011.40
101. Nery S, Vieira M, Dela Cruz C, et al. Seminal plasma concentrations of Anti-Müllerian hormone and inhibin B predict motile sperm recovery from cryopreserved semen in asthenozoospermic men: a prospective cohort study. *Andrology*. 2014;2(6):918–923. doi:10.1111/andr.278
102. Garcia TX, Farmaha JK, Kow S, Hofmann M-C. RBPJ in mouse Sertoli cells is required for proper regulation of the testis stem cell niche. *Development*. 2014;141(23):4468–4478. doi:10.1242/dev.113969
103. Rebourcet D, Darbey A, Monteiro A, et al. Sertoli cell number defines and predicts germ and Leydig cell population sizes in the adult mouse testis. *Endocrinology*. 2017;158(9):2955–2969. doi:10.1210/en.2017-00196
104. Haque R, Bin-Hafeez B, Ahmad I, Parvez S, Pandey S, Raisuddin S. Protective effects of Emblica officinalis Gaertn. in cyclophosphamide-treated mice. *Hum Exp Toxicol*. 2001;20(12):643–650. doi:10.1191/096032701718890568
105. Das UB, Mallick M, Debnath JM, Ghosh D. Protective effect of ascorbic acid on cyclophosphamide-induced testicular gametogenic and androgenic disorders in male rats. *Asian J Androl*. 2002;4(3):201–208.
106. Ghosh D, Das U, Ghosh S, Mallick M, Debnath J. Testicular gametogenic and steroidogenic activities in cyclophosphamide treated rat: a correlative study with testicular oxidative stress. *Drug Chem Toxicol*. 2002;25(3):281–292. doi:10.1081/DCT-120005891
107. Trasler JM, Hermo L, Robaire B. Morphological changes in the testis and epididymis of rats treated with cyclophosphamide: a quantitative approach. *Biol Reprod*. 1988;38(2):463–479. doi:10.1095/biolreprod38.2.463
108. Trasler JM, Hales BF, Robaire B. Chronic low dose cyclophosphamide treatment of adult male rats: effect on fertility, pregnancy outcome and progeny. *Biol Reprod*. 1986;34(2):275–283. doi:10.1095/biolreprod34.2.275
109. Qureshi M, Pennington J, Goldsmith H, Cox P. Cyclophosphamide therapy and sterility. *Lancet*. 1972;300(7790):1290–1291. doi:10.1016/S0140-6736(72)92657-8
110. Howell SJ, Shalet SM. Spermatogenesis after cancer treatment: damage and recovery. *JNCi Monographs*. 2005;2005(34):12–17. doi:10.1093/jncimonographs/lgi003
111. Goldberg MA, Antin JH, Guinan EC, Rappeport JM. Cyclophosphamide cardiotoxicity: an analysis of dosing as a risk factor. *Blood*. 1986;68(5):1114–1118. doi:10.1182/blood.V68.5.1114.1114.
112. Aitken R, Clarkson J. Cellular basis of defective sperm function and its association with the genesis of reactive oxygen species, lipid peroxidation and human sperm function. *J Reprod Fertil*. 1987;41:183–197.